Radiative Transfer Equation and Solutions 23

Junming M. Zhao and Linhua H. Liu

Contents

Abstract

Radiative transfer equation (RTE) is the governing equation of radiation propagation in participating media, which plays a central role in the analysis of radiative transfer in gases, semitransparent liquids and solids, porous materials, and particulate media, and is important in many scientific and engineering disciplines. There are different forms of RTEs that are suitable for different

J. M. Zhao (✉) · L. H. Liu
School of Energy Science and Engineering, Harbin Institute of Technology, Harbin, China
e-mail: jmzhao@hit.edu.cn; lhliu@hit.edu.cn

© Springer International Publishing AG, part of Springer Nature 2018

F. A. Kulacki (ed.), *Handbook of Thermal Science and Engineering*,
https://doi.org/10.1007/978-3-319-26695-4_56

applications, including the RTE under different coordinate systems, the transformed RTE having good numerical properties, the RTE for refractive media, etc. This chapter gives a comprehensive overview and introduction of the different forms of RTEs. Furthermore, several fundamental numerical methods for solving RTEs are introduced with the focus on the deterministic methods, such as the spherical harmonics method, discrete-ordinate method, finite volume method, and finite element method. The understanding of the numerical errors for solving the RTEs, including their origin and effects on numerical results, and the related accuracy improvement strategies are reviewed and discussed.

1 Introduction

Radiative transfer equation is the governing equation of radiation propagation in participating media, which describes the general balance of radiative energy transport in the participating media taking into account the interactions of attenuation and augmentation by absorption, scattering, and emission processes (Howell et al. 2011; Modest 2013). The equations of radiative transfer play a central role in the analysis of radiative transfer in gases, semitransparent liquids and solids, porous materials, and particulate media, which are important in many scientific and engineering disciplines, such as combustion systems (Viskanta and Mengüç 1987; Modest and Haworth 2016), rockets (Simmons 2000), atmospheric radiation (Liou 2002), remote sensing, astrophysics, noncontact temperature field measurement (Zhou et al. 2005), optical tomography (Klose et al. 2002), photo-bioreactors (Pilon et al. 2011; Berberoglu et al. 2007), and solar energy harvesting (Benoit et al. 2016; Agrafiotis et al. 2007; Mahian et al. 2013).

The classical equation of radiative transfer is a first-order integral-differential equation describing radiative energy transport in media with uniform refractive index, i.e., light beam propagates through straight lines in the media. It has been widely applied to radiative transfer analysis in scientific and engineering problems and demonstrated to be a reliable theory for engineering applications. There are many variant forms of radiative transfer equations. For example, in order for convenience of solution for specific problems, the equations of radiative transfer are usually formulated under different coordinate systems and shown in different forms, such as Lagrange form in ray-path coordinate and Eulerian forms in common orthogonal coordinate systems, Cartesian coordinate system and cylindrical coordinate system, etc. Furthermore, the traditional form of radiative transfer equations, namely, the first-order integral-differential equation, can be transformed to second-order forms to improve stability for numerical solution, such as the even-parity formulation of radiative transfer equation (Song and Park 1992) and the second-order radiative transfer equations (Zhao et al. 2013; Zhao and Liu 2007a). However, due to the structural characteristics of a material or a possible temperature/pressure dependency, the refractive index of a medium may be a function of spatial position. Some examples of participating media with gradient refractive index distribution are

earth's (or other planets') atmosphere, the ocean water, the hot air/gas of a flame, and artificial materials, such as graded index lens, graded index optical fiber, etc. In such cases, the classical equation of radiative transfer has to be extended to take into account the effect of curved ray path, resulting in the equation of radiative transfer in refractive media (Liu and Tan 2006). Radiative transfer in graded index media has attracted the interest of many researchers; some recent works include Refs. Asllanaj and Fumeron (2010), Wu and Hou (2012), Zhang et al. (2012), Hou et al. (2015), Chai et al. (2015), and Huang et al. (2016), to name a few.

Numerical simulation is crucial to analyze radiative transfer in real applications, since analytical solutions exist only for a few simple cases due to the mathematical complexity of radiative transfer equation and the complex configuration of the problems. However, numerical simulation of radiative transfer in participating media is usually time consuming and requires considerable effort due to the complexity and the high dimensionality of radiative transfer process, which contains additional dimensions of one frequency and two angular dimensions besides the common three spatial dimensions. Hence efficient and accurate numerical methods are very important for most practical applications. Many efforts have been devoted to devise effective methods for the analysis of radiative transfer in participating media. Until recently, many numerical methods have been developed for the solution of radiative transfer equation. Generally, the methods can be classified into two groups, the first group is based on stochastic simulation, which includes various implementation of Monte Carlo methods (MCM) (Howell 1968; Farmer and Howell 1994; Siegel and Howell 2002) and the DESOR method (Zhou and Cheng 2004), and the second group is the deterministic methods, such as spherical harmonics method (or P_N approximation) (Mengüç and Viskanta 1985; Larsen et al. 2002), discrete-ordinate methods (DOM) (Carlson and Lathrop 1965; Fiveland 1988; Coelho 2002a), finite volume method (FVM) (Raithby and Chui 1990; Chai and Lee 1994; Murthy and Mathur 1998; Asllanaj and Fumeron 2010), finite element method (FEM) (Liu et al. 2008), radiation element method (Maruyama 1993), spectral element method (Zhao and Liu 2006), spectral methods (Li et al. 2008), and meshless methods (Sadat 2006; Liu and Tan 2007), to name a few. A review of numerical methods for solving the RTE refers to the textbook by Modest (2013).

As being approximate methods, all numerical methods suffer several kinds of numerical errors. The MC method suffers from statistic errors. The DOM, FVM, and FEM suffer from space and angular discretization errors. The significance of numerical errors is problem dependent. It will add unphysical features to the solution to make the solution difficult to be interpreted and may sometimes totally spoil the solution. Hence to know the origin and characteristics of numerical errors is important, which can help to interpret the results of numerical simulation and to design strategies to reduce or eliminate the errors. It has been known for decades that DOM method suffers two kinds of numerical errors, i.e., false scattering and ray effects, and several strategies have been proposed to reduce these errors (Chai et al. 1993). Since the FVM can be considered a DOM with a special angular quadrature scheme, FEM and many other methods are based on the discrete-ordinate equations. Thus the

false scattering and ray effects are two general kinds of numerical errors, which need to be thoroughly understood. Recently, Hunter and Guo (2015) gave a comprehensive analysis on the numerical errors on solution of RTE.

In this chapter, the classical radiative transfer equation and several variant forms of radiative transfer equation, different solution techniques for the radiative transfer equations, numerical errors on the solution of radiative transfer equation, and the related improvement strategies are presented and discussed. The chapter is organized as follows. Firstly, the classical radiative transfer equation and variant forms of radiative transfer equation are presented in Sect. 2. Then, the different solution techniques for the radiative transfer equation are introduced in Sect. 3. Finally, the numerical errors on the solution of radiative transfer equation and the related improvement strategies are presented in Sect. 4.

2 Radiative Transfer Equation

In this section, the governing equations of radiative transfer, including the classic radiative transfer equation, the radiative transfer equation in refractive media, and the different variant forms of the radiative transfer equations, are introduced.

2.1 The Classical Radiative Transfer Equation (RTE)

The classical equation of radiative transfer describes the balance radiative energy transport in absorbing, emitting, and scattering media with uniform refractive index distribution. Generally, the radiative power of a light beam in the medium is a function of wavelength λ (μm), transfer direction $\mathbf{\Omega}$, and spatial location $\mathbf{r}$, which is described using the physical quantity of radiative intensity $I_\lambda(\mathbf{r}, \mathbf{\Omega})$. It has unit W/(m^{2}μm sr), denoting the transferred radiative power per unit cross-section area along the transfer direction, per wavelength, and per solid angle. The RTE is a governing equation of radiative intensity $I_\lambda(\mathbf{r}, \mathbf{\Omega})$. In the following, the RTE in different coordinate system, the energy relations, and the numerical property of RTE are presented.

2.1.1 Ray-Path Coordinate System Formulation

Ray-path coordinate is the natural coordinate system for light transfer. Here the RTE is formulated in the one-dimensional Lagrangian ray-path coordinate at first. The Lagrangian form of RTE is the physical clearest, in the simplest mathematical form, and considered to be the most general formulation such that the RTE under other different coordinate systems can be derived just by expressing the stream operator under the system.

A control volume in cylinder shape along the ray path between s and $s + ds$ is considered as shown in Fig. 1. A light beam enters the left surface at s and exits at $s + ds$. The end surface of the cylinder is perpendicular to the ray transfer direction $\mathbf{s}$ with an area of dA. The radiative intensity along the ray-path direction can be

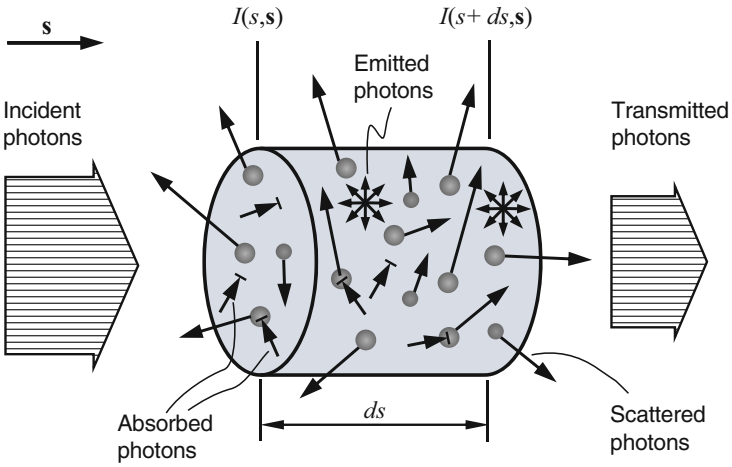

Fig. 1 Schematic of light transport in participating medium. The photon beam is attenuated by absorption and out-scattering and augmented by emission and in-scattering processes

expressed as $I_\lambda(s, \mathbf{s})$. At the same location, the radiative intensity of any other direction $\mathbf{\Omega}$ can be expressed as $I_\lambda(s, \mathbf{\Omega})$. When the light beam (photons) moves from location s to $s + ds$, the balance of spectral radiative power Q_λ (W) can be expressed as follows:

$$\Delta Q_\lambda = \underbrace{\left(\Delta Q_{\lambda,\,\mathrm{abs}} + \Delta Q_{\lambda,\,\mathrm{out\text{-}scatt}}\right)}_{\text{Attenuation}} + \underbrace{\left(\Delta Q_{\lambda,\,\mathrm{emit}} + \Delta Q_{\lambda,\,\mathrm{in\text{-}scatt}}\right)}_{\text{Augmentation}} \tag{1}$$

where ΔQ_λ denotes the variation of spectral radiative power along the differential ray-path ds, which can be calculated by definition as $\Delta Q_\lambda = [I_\lambda(s + ds, \mathbf{s}) - I_\lambda(s, \mathbf{s})]\, dAd\Omega$, $d\Omega$ is a differential solid angle, and the four terms at right-hand side indicate the contributions of the basic interaction mechanisms in participating media, namely, absorption ($\Delta Q_{\lambda,\,\mathrm{abs}}$), scattering ($\Delta Q_{\lambda,\,\mathrm{out\text{-}scatt}}$ and $\Delta Q_{\lambda,\,\mathrm{in\text{-}scatt}}$), and emission processes ($\Delta Q_{\lambda,\,\mathrm{emit}}$). Absorption process transfers the radiative power to kinetic energy of heat carriers (e.g., electrons and phonons), which only attenuates the radiative power. Thermal emission process only augments the radiative power. As for the scattering process, it can both attenuate and augment the radiative power depending on whether it is the scattering of the current light beam $I_\lambda(s, \mathbf{s})$ to other directions, i.e., the out-scattering process, or the scattering of light beam of other direction $I_\lambda(s, \mathbf{\Omega})$ to current transfer direction $\mathbf{s}$, i.e., the in-scattering process.

The attenuated radiative power in the control volume is proportional to the incident radiative power, which for the processes of absorption and out-scattering can be established respectively as

$$\Delta Q_{\lambda,\,\mathrm{abs}} = -\kappa_{a,\lambda} I_\lambda(s, \mathbf{s}) dsdAd\Omega, \quad \Delta Q_{\lambda,\,\mathrm{out\text{-}scatt}} = -\kappa_{s,\lambda} I_\lambda(s, \mathbf{s}) dsdAd\Omega \tag{2}$$

where $\kappa_{a,\lambda}$ (m^{-1}) and $\kappa_{s,\lambda}$ (m^{-1}) are the spectral *absorption coefficient* and *scattering coefficient*, respectively. The emitted radiative power in the control volume is established based on the black body radiative intensity as

$$\Delta Q_{\lambda,\,\mathrm{abs}} = \kappa_{a,\lambda} I_{b,\lambda}[T(s)] ds dA d\Omega \tag{3}$$

in which Kirchhoff's law of thermal radiation is applied, $\kappa_{a,\lambda} ds$ can be viewed as the emissivity of the layer of medium with thickness ds, and $I_{b,\,\lambda}$ is the black body spectral radiative intensity. For a black body in a transparent medium with refractive index n_λ, $I_{b,\,\lambda}$ is calculated from (Modest 2013)

$$I_{b,\lambda} = n_\lambda^2 I_{b,\lambda}^0 = \frac{2hc^2 n_\lambda^2}{\lambda^5 (e^{hc/\lambda k_B T} - 1)} \tag{4}$$

where $I_{b,\lambda}^0$ is the radiative intensity of black body in vacuum, $c = 2.998 \times 10^8$ (m/s) is vacuum light speed, $h = 6.626 \times 10^{-34}$ (J s) is the Planck's constant, and $k_B = 1.3807 \times 10^{-23}$ (J/K) is the Boltzmann's constant. Note that the wavelength λ denotes vacuum wavelength throughout this text.

The scattering process generally changes the direction of incident photons. This angular redistribution of incident photons by scattering process is described by the *scattering phase function*, which expresses the ratio of radiative power scattered to each direction per solid angle. By definition, the scattering phase function $\Phi_\lambda(\cos\Theta)$ (sr^{-1}) must satisfy scattering energy conservation, which is often called normalization relation and written as

$$\frac{1}{4\pi} \int_{4\pi} \Phi_\lambda(\cos\Theta) d\Omega = 1 \tag{5}$$

where $\cos\Theta = \mathbf{\Omega}' \cdot \mathbf{\Omega}$ is the cosine of the angle between incident ($\mathbf{\Omega}'$) and scattering direction ($\mathbf{\Omega}$). For a light beam with radiative intensity $I_\lambda(\mathbf{\Omega}', \mathrm{s})$ incident on a differential control volume with volume dV, the total scattered radiative power by the scatterers in the control volume is $\kappa_{s,\lambda} I_\lambda(\mathbf{\Omega}', \mathrm{s}) dV d\Omega'$ according to Eq. (2), where $d\Omega'$ is a differential solid angle related to the incident beam of direction $\mathbf{\Omega}'$. Then the scattered power from an arbitrary incident direction $\mathbf{\Omega}'$ to the current transfer direction $\mathbf{s}$ is $\kappa_{s,\lambda} I_\lambda(s, \mathbf{\Omega}') \frac{1}{4\pi} \Phi_\lambda(\mathbf{\Omega}' \cdot \mathbf{s}) dV d\Omega' d\Omega$. The total in-scattering radiative power augmentation from all directions can then be calculated by integration as

$$\Delta Q_{\lambda,\,\text{in-scatt}} = \frac{\kappa_{s,\lambda}}{4\pi} \int_{4\pi} I_\lambda(s, \mathbf{\Omega}') \Phi_\lambda(\mathbf{\Omega}' \cdot \mathbf{s}) d\Omega' ds dA d\Omega \tag{6}$$

By substitution of Eqs. (3), (2), and (6) into Eq. (1), the Lagrangian form of RTE can be obtained as

$$\frac{\mathrm{d}I_\lambda(s,\mathbf{s})}{\mathrm{d}s}+\beta_\lambda I_\lambda(s,\mathbf{s})=\kappa_{a,\lambda}I_{b,\lambda}[T(s)]+\frac{\kappa_{s,\lambda}}{4\pi}\int_{4\pi}I_\lambda(s,\mathbf{\Omega}')\Phi_\lambda(\mathbf{\Omega}'\cdot\mathbf{s})\mathrm{d}\Omega' \tag{7}$$

where $\beta_\lambda = (\kappa_{a,\lambda} + \kappa_{s,\lambda})$ is the extinction coefficient. If the ray coordinate is not moved with beam propagation, namely, Eulerian frame is used. The radiative intensity will be function of time t, and the fixed ray coordinate s can be expressed as $I_\lambda(s, t, \mathbf{s})$. In this case, the Lagrangian stream operator d/ds can be expanded as

$$\frac{\mathrm{d}}{\mathrm{d}s}=\frac{\partial}{\partial s}+\frac{\partial}{\partial t}\frac{dt}{ds}=\frac{\partial}{\partial s}+\frac{n_\lambda}{c}\frac{\partial}{\partial t} \tag{8}$$

where c is the light speed in vacuum. Using Eq. (8), the RTE can be expressed in Eulerian form as

$$\begin{aligned}\frac{n_\lambda}{c}\frac{\partial I_\lambda(s,t,\mathbf{s})}{\partial t}+\frac{\partial I_\lambda(s,t,\mathbf{s})}{\partial s}+\beta_\lambda I_\lambda(s,t,\mathbf{s})\\ =\kappa_{a,\lambda}I_{b,\lambda}[T(s)]+\frac{\kappa_{s,\lambda}}{4\pi}\int_{4\pi}I_\lambda(s,t,\mathbf{\Omega}')\Phi_\lambda(\mathbf{\Omega}'\cdot\mathbf{s})\mathrm{d}\Omega'\end{aligned} \tag{9}$$

Equations (7) and (9) are the basic form of RTEs in uniform refractive index media. As can be seen, for steady-state radiative transfer, Eqs. (7) and (9) are the same. Equation (9) is specially useful for transient radiative transfer analysis. The RTEs in other coordinate systems can be derived by simply expressing the stream operator in the coordinate system. In the following, only steady-state RTE is considered unless otherwise mentioned.

2.1.2 Cartesian Coordinate System Formulation

In Cartesian coordinate system, radiative intensity is expressed as $I_\lambda(s(x, y, z), \mathbf{\Omega})$; hence,

$$\frac{\mathrm{d}I}{\mathrm{d}s}=\frac{\mathrm{d}x}{\mathrm{d}s}\frac{\partial I}{\partial x}+\frac{\mathrm{d}y}{\mathrm{d}s}\frac{\partial I}{\partial y}+\frac{\mathrm{d}z}{\mathrm{d}s}\frac{\partial I}{\partial z} \tag{10}$$

Considering ds as the arc length along a curve, the coordinate transformation coefficients dx/ds, dy/ds, and dz/ds are the direction cosines of the transport direction $\mathbf{\Omega} = \mu\mathbf{i} + \eta\mathbf{j} + \xi\mathbf{k}$. As such, Eq. (10) can be written as

$$\frac{\mathrm{d}I}{\mathrm{d}s}=\mu\frac{\partial I}{\partial x}+\eta\frac{\partial I}{\partial y}+\xi\frac{\partial I}{\partial z}=\mathbf{\Omega}\cdot\nabla I \tag{11}$$

The RTE in Cartesian coordinate system can then be written as

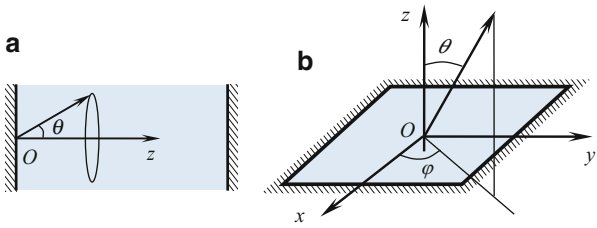

Fig. 2 1D and 2D Cartesian system with variable defined to formulate the RTE. (**a**) 1D and (**b**) 2D

$$\boldsymbol{\Omega}\cdot\nabla I_\lambda(\mathbf{r},\boldsymbol{\Omega})+\beta_\lambda I_\lambda(\mathbf{r},\boldsymbol{\Omega})=\kappa_a,\ {}_\lambda I_b,\ {}_\lambda[T(\mathbf{r})]+\frac{\kappa_{s,\ \lambda}}{4\pi}\times\int_{4\pi}I_\lambda(\mathbf{r},\boldsymbol{\Omega}')\Phi_\lambda(\boldsymbol{\Omega}'\cdot\boldsymbol{\Omega})\mathrm{d}\Omega' \tag{12}$$

where $\mathbf{r}=x\mathbf{i}+y\mathbf{j}+z\mathbf{k}$ is the spatial location vector.

For 1D and 2D cases, the equation can be simplified by employing the symmetries of radiative intensity distribution, i.e., the axisymmetric around z-axis for 1D and mirror symmetry about z-axis for the 2D case as shown in Fig. 2. The 1D RTE can be written as

$$\xi\frac{\mathrm{d}I_\lambda(\mathrm{z},\xi)}{\mathrm{d}z}+\beta_\lambda I_\lambda(\mathrm{z},\xi)=\kappa_{a,\lambda}I_{b,\lambda}[T(z)]+\int_{-1}^{1}I(\mathrm{z},\xi')\Phi_{1,\lambda}(\xi',\xi)\mathrm{d}\xi' \tag{13}$$

where $\xi=\cos\theta$, $\Phi_{1,\lambda}(\xi',\xi)=\frac{1}{2\pi}\int_0^{2\pi}\Phi(\boldsymbol{\Omega}'\cdot\boldsymbol{\Omega})\mathrm{d}\varphi$ is the 1D scattering phase function. The scattering phase function can be expanded in Legendre polynomials P_m as

$$\Phi(\boldsymbol{\Omega}'\cdot\boldsymbol{\Omega})=\Phi(\cos\Theta)=1+\sum_{m=1}^{M}A_mP_m(\cos\Theta) \tag{14}$$

where A_m is the m-th order expansion coefficients. Then the 1D scattering phase function can be expressed as (Modest 2013)

$$\Phi_{1,\lambda}(\xi',\xi)=1+\sum_{m=1}^{M}A_mP_m(\xi')P_m(\xi) \tag{15}$$

For the 2D case, the mirror symmetry indicates $I(\boldsymbol{\Omega},\mathbf{r})=I\left(\overline{\boldsymbol{\Omega}},\mathbf{r}\right)$, where $\overline{\boldsymbol{\Omega}}_m=[\mu,\eta,\ -\xi]$; hence, the RTE can be written as (Zhao et al. 2013)

$$\mu\frac{\partial I_\lambda}{\partial x}+\eta\frac{\partial I_\lambda}{\partial y}+\beta_\lambda I_\lambda\ =\kappa_{a,\lambda}I_{b,\lambda}+\frac{\kappa_{s,\lambda}}{4\pi}\int_{2\pi}I_\lambda(\mathbf{r},\boldsymbol{\Omega}')\Phi_{2,\lambda}(\boldsymbol{\Omega}'\cdot\boldsymbol{\Omega})\mathrm{d}\Omega' \tag{16}$$

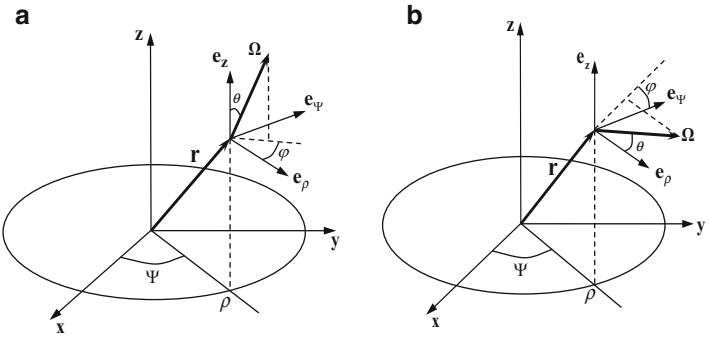

Fig. 3 Definition of the cylindrical coordinate system. (**a**) Type I and (**b**) Type II

where $\Phi_{2,\lambda}(\mathbf{\Omega}' \cdot \mathbf{\Omega}) = \Phi_\lambda(\mathbf{\Omega}' \cdot \mathbf{\Omega}) + \Phi_\lambda\left(\overline{\mathbf{\Omega}'} \cdot \mathbf{\Omega}\right)$ is the 2D scattering phase function, and the angular quadrature is only over half solid angular space at $\theta \in [0, \pi/2]$.

2.1.3 RTE in Other Coordinate Systems

Besides the Cartesian coordinate system, cylindrical and spherical coordinate systems are the other two commonly used orthogonal coordinate systems. Here the RTE in these coordinate systems is presented. Currently, two types of cylindrical coordinate system (ρ-Ψ-z-θ-φ) were proposed for radiative transfer analysis in literatures, whose definitions are shown in Fig. 3. The Type I cylindrical coordinate system is the traditional one (Modest 2013), and the Type II cylindrical coordinate system is a relatively new one proposed recently (Zhang et al. 2010). The difference between these two systems lies in the definition of local angular variables, i.e., the zenith angle θ and azimuthal angle φ. By definition, the optical plane of reflection or refraction at the cylindrical interfaces coincides with the iso-surface of azimuthal angle φ in the Type II system; hence, it facilitates the treatment of reflection/refraction at the cylindrical interfaces/boundaries.

For the Type I cylindrical coordinate system (Fig. 3a), the stream operator d/ds can be expanded as (Modest 2013)

$$\begin{aligned}\frac{d}{ds} &= \frac{d\rho}{ds}\frac{\partial}{\partial\rho} + \frac{d\Psi}{ds}\frac{\partial}{\partial\Psi} + \frac{dz}{ds}\frac{\partial}{\partial z} + \frac{d\theta}{ds}\frac{\partial}{\partial\theta} + \frac{d\varphi}{ds}\frac{\partial}{\partial\varphi} \\ &= \mathbf{\Omega}\cdot\nabla_{\mathrm{I}} - \frac{\eta}{\rho}\frac{\partial}{\partial\varphi}\end{aligned} \tag{17}$$

where $\mathbf{\Omega} = \mu\mathbf{e}_\rho + \eta\mathbf{e}_\Psi + \xi\mathbf{e}_z$ is the local direction vector of the beam; $\mu = \sin\theta\cos\varphi$; $\eta = \sin\theta\sin\varphi$; $\xi = \cos\theta$; $\mathbf{e}_\rho$, $\mathbf{e}_\Psi$, and $\mathbf{e}_z$ are the unit coordinate vector; and $\nabla_{\mathrm{I}} = \mathbf{e}_\rho\partial/\partial\rho + \mathbf{e}_\Psi\rho^{-1}\partial/\partial\Psi + \mathbf{e}_z\partial/\partial z$ is the gradient operator in the Type I cylindrical coordinate system. Hence the RTE in the Type I cylindrical coordinate system can be written as

$$\boldsymbol{\Omega}\cdot\nabla I_\lambda-\frac{\eta}{\rho}\frac{\partial I_\lambda}{\partial\varphi}+\beta_\lambda I_\lambda=\kappa_{a,\lambda}I_{b,\lambda}+\frac{\kappa_{s,\lambda}}{4\pi}\int_{4\pi}I_\lambda(\mathbf{r},\boldsymbol{\Omega}')\Phi_\lambda(\boldsymbol{\Omega}'\cdot\boldsymbol{\Omega})\mathrm{d}\Omega' \tag{18}$$

This is in nonconservative form, and it can be further rewritten in conservative form as

$$\boldsymbol{\Omega}\cdot\widetilde{\nabla}_{\mathrm{I}}I_\lambda-\frac{1}{\rho}\frac{\partial\eta I_\lambda}{\partial\varphi}+\beta_\lambda I_\lambda=\kappa_{a,\lambda}I_{b,\lambda}+\frac{\kappa_{s,\lambda}}{4\pi}\int_{4\pi}I_\lambda(\mathbf{r},\boldsymbol{\Omega}')\Phi_\lambda(\boldsymbol{\Omega}'\cdot\boldsymbol{\Omega})\mathrm{d}\Omega' \tag{19}$$

where $\widetilde{\nabla}_{\mathrm{I}}(\cdot)=\mathbf{e}_\rho\rho^{-1}\,\partial\,(\rho\cdot)/\,\partial\rho+\mathbf{e}_\Psi\rho^{-1}\,\partial\,(\cdot)/\,\partial\Psi+\mathbf{e}_z\rho^{-1}\,\partial\,(\cdot)/\,\partial z$ is a modified gradient operator in the Type I cylindrical coordinate system.

For the Type II cylindrical coordinates system (Fig. 3b), the stream operator can be expanded as (Zhang et al. 2010; Zhao et al. 2012b)

$$\frac{d}{ds}=\boldsymbol{\Omega}\cdot\nabla_{\mathrm{II}}-\mu\frac{\cos\varphi}{\rho}\frac{\partial}{\partial\theta}+\xi\frac{\sin\varphi\cos\varphi}{\rho}\frac{\partial}{\partial\varphi} \tag{20}$$

where $\boldsymbol{\Omega}=\mu\mathbf{e}_\Psi+\eta\mathbf{e}_z+\xi\mathbf{e}_\rho$ is the local direction vector of the beam and the gradient operator is given as $\nabla_{\mathrm{II}}=\mathbf{e}_\Psi\rho^{-1}\partial/\partial\Psi+\mathbf{e}_z\partial/\partial z+\mathbf{e}_\rho\partial/\partial\rho$. The RTE in the Type II cylindrical coordinate system can thus be written as

$$\begin{aligned}\boldsymbol{\Omega}\cdot\nabla_{\mathrm{II}}I_\lambda-\mu\frac{\cos\varphi}{\rho}\frac{\partial I_\lambda}{\partial\theta}+\xi\frac{\sin\varphi\cos\varphi}{\rho}\frac{\partial I_\lambda}{\partial\varphi}+\beta_\lambda I_\lambda\\=\kappa_{a,\lambda}I_{b,\lambda}+\frac{\kappa_{s,\lambda}}{4\pi}\int_{4\pi}I_\lambda(\mathbf{r},\boldsymbol{\Omega}')\Phi_\lambda(\boldsymbol{\Omega}'\cdot\boldsymbol{\Omega})\mathrm{d}\Omega'\end{aligned} \tag{21}$$

This is in nonconservative form, and it can be further rewritten in conservative form as

$$\begin{aligned}&\boldsymbol{\Omega}\cdot\widetilde{\nabla}_{\mathrm{II}}I_\lambda-\frac{1}{\rho\sin\theta}\frac{\partial}{\partial\theta}\left[\mu^2I_\lambda\right]+\frac{1}{\rho}\frac{\partial}{\partial\varphi}\left[\xi\sin\varphi\cos\varphi I_\lambda\right]+\beta_\lambda I_\lambda\\&=\kappa_{a,\lambda}I_{b,\lambda}+\frac{\kappa_{s,\lambda}}{4\pi}\int_{4\pi}I_\lambda(\mathbf{r},\boldsymbol{\Omega}')\Phi_\lambda(\boldsymbol{\Omega}'\cdot\boldsymbol{\Omega})\mathrm{d}\Omega'\end{aligned} \tag{22}$$

where $\widetilde{\nabla}_{\mathrm{II}}(\cdot)=\mathbf{e}_\Psi\rho^{-1}\,\partial\,(\cdot)/\,\partial\Psi+\mathbf{e}_z\,\partial\,(\cdot)/\,\partial z+\mathbf{e}_\rho\rho^{-1}\,\partial\,(\rho\cdot)/\,\partial\rho$ is a modified gradient operator.

For the spherical coordinate system (Θ-Ψ-ρ-θ-φ) defined in Fig. 4, the stream operator can be expanded as (Liu et al. 2008)

$$\begin{aligned}\frac{d}{ds}&=\frac{d\Theta}{ds}\frac{\partial}{\partial\Theta}+\frac{d\Psi}{ds}\frac{\partial}{\partial\Psi}+\frac{d\rho}{ds}\frac{\partial}{\partial\rho}+\frac{d\theta}{ds}\frac{\partial}{\partial\theta}+\frac{d\varphi}{ds}\frac{\partial}{\partial\varphi}\\&=\boldsymbol{\Omega}\cdot\nabla-\frac{\sin\theta}{\rho}\frac{\partial}{\partial\theta}-\frac{\eta\cot\Theta}{\rho}\frac{\partial}{\partial\varphi}\end{aligned} \tag{23}$$

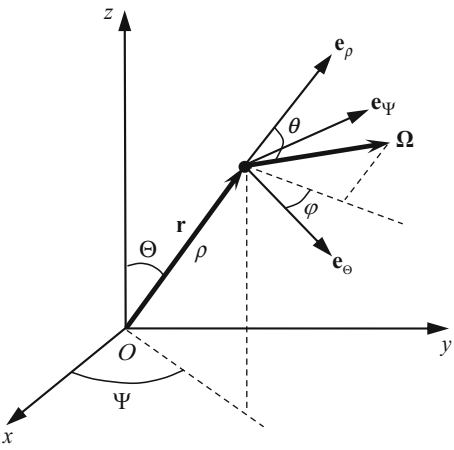

Fig. 4 Definition of the spherical coordinate system

where $\mathbf{\Omega} = \mu\mathbf{e}_\Theta + \eta\mathbf{e}_\Psi + \xi\mathbf{e}_\rho$ is the local direction vector of the beam and the gradient operator is defined as $\nabla = \mathbf{e}_\Theta\rho^{-1}\partial/\partial\Theta + \mathbf{e}_\Psi(\rho\sin\Theta)^{-1}\partial/\partial\Psi + \mathbf{e}_\rho\partial/\partial\rho$. The RTE in the spherical coordinate system can be obtained in the nonconservative form as

$$\begin{aligned}\mathbf{\Omega}\cdot\nabla I_\lambda - \frac{\sin\theta}{\rho}\frac{\partial I_\lambda}{\partial\theta} - \frac{\eta\cot\Theta}{\rho}\frac{\partial I_\lambda}{\partial\varphi} + \beta_\lambda I_\lambda \\ = \kappa_{a,\lambda}I_{b,\lambda} + \frac{\kappa_{s,\lambda}}{4\pi}\int_{4\pi} I_\lambda(\mathbf{r},\mathbf{\Omega}')\Phi_\lambda(\mathbf{\Omega}'\cdot\mathbf{\Omega})\mathrm{d}\Omega'\end{aligned} \tag{24}$$

and in the conservative form as

$$\begin{aligned}&\mathbf{\Omega}\cdot\widetilde{\nabla} I_\lambda - \frac{1}{\rho\sin\theta}\frac{\partial\left(1-\xi^2\right)I_\lambda}{\partial\theta} - \frac{\cot\Theta}{\rho}\frac{\partial\eta I_\lambda}{\partial\varphi} + \beta_\lambda I_\lambda \\ &= \kappa_{a,\lambda}I_{b,\lambda} + \frac{\kappa_{s,\lambda}}{4\pi}\int_{4\pi} I_\lambda(\mathbf{r},\mathbf{\Omega}')\Phi_\lambda(\mathbf{\Omega}'\cdot\mathbf{\Omega})\mathrm{d}\Omega'\end{aligned} \tag{25}$$

where $\widetilde{\nabla}(\cdot) = \mathbf{e}_\Theta(\rho\sin\Theta)^{-1}\,\partial\,(\sin\Theta\,\cdot)/\,\partial\Theta + \mathbf{e}_\Psi(\rho\sin\Theta)^{-1}\,\partial\,/\,\partial\Psi + \mathbf{e}_\rho\rho^{-2}\,\partial\,(\rho^2\cdot)/\,\partial\rho$ is a modified gradient operator.

2.1.4 Overall Energy Conservation

If the radiative intensity is known, then any other derived quantities such as radiative heat flux vector, incident radiation, radiation energy density, volumetric radiation source term (or divergence of radiative heat flux vector), absorbed radiative power per unit volume, etc. can be readily calculated. The radiative heat flux vector $\mathbf{q}_\lambda$ (W/(m^{2}μm)) and incident radiation G (W/(m^{2}μm)) are calculated based on radiative intensity as

$$\mathbf{q}_\lambda(\mathbf{r}) = \int_{4\pi} I_\lambda(\mathbf{r}, \mathbf{\Omega})\mathbf{\Omega} d\Omega, \quad G_\lambda(\mathbf{r}) = \int_{4\pi} I_\lambda(\mathbf{r}, \mathbf{\Omega}) d\Omega \tag{26}$$

The total radiative heat flux vector $\mathbf{q}$ and total incident radiation G can be calculated by a spectral integration with wavelength to $\mathbf{q}_\lambda$ and G_λ, respectively. The net spectral radiative heat flux onto a surface element $q_{s,\lambda}$ (W/(m^{2}μm)) can thus be calculated from $q_{s,\lambda} = \mathbf{q}_\lambda \cdot \mathbf{n}_w$. The spectral radiation energy density u_λ (J/(m^{3}μm)) is

$$u_\lambda(\mathbf{r}) = \frac{n_\lambda}{c} \int_{4\pi} I_\lambda(\mathbf{r}, \mathbf{\Omega}) d\Omega = \frac{n_\lambda}{c} G_\lambda(\mathbf{r}) \tag{27}$$

The absorbed spectral radiative power per unit volume w_λ (W/(m^{3}μm)) can be calculated from

$$w_\lambda(\mathbf{r}) = \kappa_a G_\lambda(\mathbf{r}) \tag{28}$$

The balance equation of spectral radiative heat flux can be obtained by integration of the RTE in Cartesian coordinates in Eq. (12) over entire solid angle, that is,

$$\nabla \cdot \mathbf{q}_\lambda = 4\pi\kappa_{a,\lambda} I_{b,\lambda} - \kappa_{a,\lambda} G_\lambda \tag{29}$$

The left-hand side of Eq. (29), namely, $\nabla \cdot \mathbf{q}_\lambda$, stands for the outflow radiation power per unit volume, which is thus can be understood as a volumetric radiation source term. The first term and the second term of the right-hand side are the emitted radiation power and the absorbed radiation power per unit volume, respectively. Balance equation of total radiative heat flux can be obtained as

$$\nabla \cdot \mathbf{q} = \int_0^\infty \kappa_{a,\lambda} \left(4\pi I_{b,\lambda} - G_\lambda\right) d\lambda \tag{30}$$

which can be simplified for gray medium ($\kappa_{a,\lambda} = \kappa_a$ and $n_\lambda = n$ are constant) as

$$\nabla \cdot \mathbf{q} = \kappa_a (4\pi I_b - G) = \kappa_a \left(4n^2 \sigma T^4 - G\right) \tag{31}$$

where $\sigma = 5.67 \times 10^{-8}$ (W/(m^{2}K^4)) is the Stefan-Boltzmann constant.

If temperature field is to be determined, and only radiation heat transfer is considered, the equation of overall energy conservation can be written as

$$\rho C_v \frac{\partial T}{\partial t} = Q'''_{rad} = \kappa_a \left(G - 4n^2 \sigma T^4\right) \tag{32}$$

where $Q'''_{rad} = -\nabla \cdot \mathbf{q}$ (W/m^3) denotes the equivalent radiative heat source, ρ (Kg/m^3) is the density, and C_v (J/(Kg K)) is the specific heat capacity of the medium. At equilibrium, the temperature field can be determined as

$$T = \left(\frac{G}{4n^2\sigma}\right)^{\frac{1}{4}} \tag{33}$$

If combined mode heat transfer of conduction and radiation is considered, the governing equation of overall energy conservation can be written as

$$\begin{aligned} \rho C_v \frac{\partial T}{\partial t} &= \nabla \cdot (k\nabla T) + Q'''_{rad} \\ &= \nabla \cdot (k\nabla T) + \kappa_a\left(G - 4n^2\sigma T^4\right) \end{aligned} \tag{34}$$

where k (W/(m K)) is the heat conductivity of medium. If further the convection heat transfer is also considered, the overall energy conservation equation can be written as

$$\begin{aligned} \rho C_v \left(\frac{\partial T}{\partial t} + \mathbf{u} \cdot \nabla T\right) &= \nabla \cdot (k\nabla T) + Q'''_{rad} + Q'''_f \\ &= \nabla \cdot (k\nabla T) + \kappa_a\left(G - 4n^2\sigma T^4\right) + Q'''_f \end{aligned} \tag{35}$$

where $\mathbf{u}$ (m/s) is the fluid velocity vector and Q'''_f denotes the volumetric heat source other than thermal radiation, such as from viscous friction, chemical reaction, etc.

2.1.5 Boundary Conditions for RTE

The inflow radiative intensity at the boundary walls must be set before the solution of the RTE. Generally speaking, three processes contributed to the emanated radiative intensity at the boundary walls, namely, the emission, reflection, and transmission. For a diffuse emitting and reflecting opaque wall, the boundary condition can be written as

$$I_\lambda(\mathbf{r}_w, \mathbf{\Omega}) = \varepsilon_{w,\lambda} I_{b,\lambda}[T(\mathbf{r}_w)] + \frac{1 - \varepsilon_{w,\lambda}}{\pi} \int_{\mathbf{n}_w \cdot \mathbf{\Omega}' > 0} I_\lambda(\mathbf{r}_w, \mathbf{\Omega}') \left|\mathbf{n}_w \cdot \mathbf{\Omega}'\right| d\Omega', \quad \mathbf{n}_w \cdot \mathbf{\Omega} < 0 \tag{36}$$

where $\varepsilon_{w\ \lambda}$ is the wall spectral emissivity and $\mathbf{n}_w$ is the normal vector of the wall pointing outside the enclosure. The boundary condition for diffuse wall (Eq. (36)) can also be written as (Modest 2013)

$$I_\lambda(\mathbf{r}_w, \mathbf{\Omega}) = I_{b,\lambda}[T(\mathbf{r}_w)] + \frac{1 - \varepsilon_{w,\lambda}}{\pi \varepsilon_{w,\lambda}} \mathbf{q} \cdot \mathbf{n}_w, \quad \mathbf{n}_w \cdot \mathbf{\Omega} < 0 \tag{37}$$

For real opaque rough surfaces, there will be significant part of radiation reflection at the specular direction. As such, the wall reflection can be separated into a diffuse reflection part and a specular reflection part. In this case, the boundary condition can be written as

$$I_\lambda(\mathbf{r}_w, \mathbf{\Omega}) = \varepsilon_{w,\lambda} I_{b,\lambda}[T(\mathbf{r}_w)] + \frac{\rho^d_{w,\lambda}}{\pi} \int_{\mathbf{n}_w \cdot \mathbf{\Omega}' > 0} I_\lambda(\mathbf{r}_w, \mathbf{\Omega}') |\mathbf{n}_w \cdot \mathbf{\Omega}'| \, d\Omega' + \rho^s_{w,\lambda} I_\lambda(\mathbf{r}_w, \mathbf{\Omega}^s) \tag{38}$$

where $\rho^d_{w,\lambda}$ and $\rho^s_{w,\lambda}$ are the diffuse and specular reflectivity, respectively, and $\mathbf{\Omega}^s$ is the corresponding incident direction of specular reflection, which can be determined as $\mathbf{\Omega}^s = \mathbf{\Omega} - 2(\mathbf{\Omega} \cdot \mathbf{n}_w)\mathbf{n}_w$.

If an external radiative source, such as a laser, a lamp, or a solar beam, is irradiated to a medium with semitransparent walls, the boundary condition can be written as

$$I_\lambda(\mathbf{r}_w, \mathbf{\Omega}) = \varepsilon_{w,\lambda} I_{b,\lambda}[T(\mathbf{r}_w)] + \frac{\rho^d_{w,\lambda}}{\pi} \int_{\mathbf{n}_w \cdot \mathbf{\Omega}' > 0} I_\lambda(\mathbf{r}_w, \mathbf{\Omega}') |\mathbf{n}_w \cdot \mathbf{\Omega}'| \, d\Omega' + \rho^s_{w,\lambda} I_\lambda(\mathbf{r}_w, \mathbf{\Omega}^s) + \tau_{w,\lambda} I_{ext}(\mathbf{r}_w, \mathbf{\Omega}) \tag{39}$$

where $\tau_{w,\lambda}$ is spectral transmittance of the semitransparent wall and $I_{ext}(\mathbf{r}_w, \mathbf{\Omega})$ is the radiative intensity of the external source.

2.1.6 Numerical Properties of the Classical RTE

The classical RTE (Eq. (12)) can be written shortly as

$$\mathbf{\Omega} \cdot \nabla I + \beta I = S \tag{40}$$

where S is the source term accounting for thermal emission and in-scattering contribution. The wavelength subscript is omitted for brevity. The first term of the left-hand side of Eq. (40) can be seen as a convection term with a convection velocity of $\mathbf{\Omega}$, namely, μ, η, and ξ, which are taken as the velocity in x-, y-, and z- directions, respectively. Hence the RTE can be considered as a special kind of convection-diffusion equation without the diffusion term (Chai et al. 2000b). The convection-dominated property is a source of numerical instability, which may cause unphysical numerical results, and shows strong ray effects (Chai et al. 2000a).

In order for illustrating the numerical stability of the first-order RTE, Fig. 5a shows the example results solved by a finite element method discretization of the first-order RTE for a 1D case with a Gaussian-shaped emissive source at different optical thickness excerpted from Ref. Zhao and Liu (2007a). The solved radiative intensity distribution shows significant unphysical oscillations, which is a good demonstration of the instability issue caused by the convection-dominated characteristics of the RTE. Following the theoretical framework presented in Ref. Zhao et al. (2013), the solution error can be predicted in frequency domain as shown in Fig. 5b. The frequency range of the reduced frequency $\overline{\varpi} = \Delta s \varpi / 2\pi$ is plotted in [0, 0.5], where ϖ denotes the angular frequency in Fourier analysis and Δs is the grid spacing. This is based on the fact that the maximum frequency (or shortest

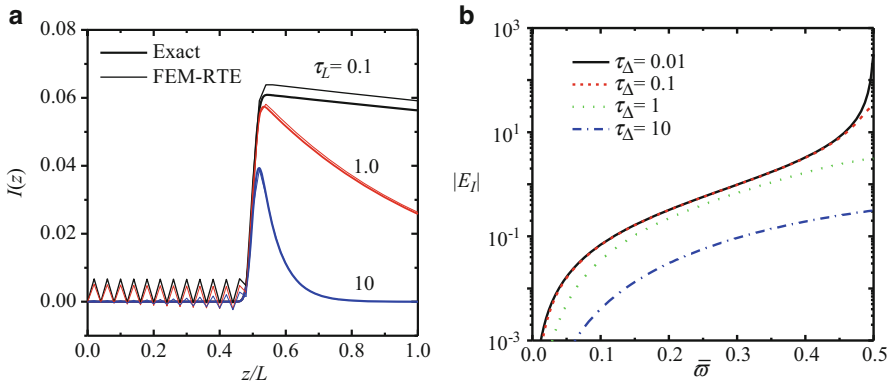

Fig. 5 Example results illustrating the numerical stability of the first-order RTE. (**a**) Intensity distribution solved by finite element method for the Gaussian-shaped emissive source problem, (**b**) theoretical frequency domain relative error of the RTE discretized using central difference scheme

wavelength) of a harmonic that can propagate on a uniform grid of spacing Δs is $\pi/\Delta s$ (or wavelength $2\Delta s$), namely, $\overline{\varpi} = 0.5$. It can be seen that the relative error of intensity $|E_I|$ increases with $\overline{\varpi}$ for different grid optical thickness and the maximum relative error occurs at $\overline{\varpi} = 0.5$ with a huge relative error greater than 300 for $\tau_\Delta =$ 0.01. Hence significant error can be observed at around $\overline{\varpi} = 0.5$, interpreting the observed high-frequency unphysical oscillations in Fig. 5a. The solution errors (especially at the high frequency) of the results obtained by the RTE reduces significantly with the increasing of grid optical thickness τ_Δ, indicating the solution error will decrease for problem with larger extinction coefficient on a specified grid, interpreting the observed decreasing of unphysical oscillations with increasing optical thickness in Fig. 5a.

2.2 The Second-Order Form of RTE

The classical form of the RTE under different coordinate systems has been presented in the previous section. The convection-dominated characteristics of the RTE may cause unphysical oscillation in the numerical results as discussed in the previous section. This type of instability occurs in many numerical methods, such as finite difference methods, finite element methods, and meshless methods, if no special stability treatment is taken (Chai et al. 2000b). It has been demonstrated that the classical RTE can be transformed to a new equation with a naturally introduced second-order diffusion term to circumvent the stability issue. In this section, several second-order form of RTEs is presented, including the even-parity formulation of RTE (EPRTE), the second-order radiative transfer equation (SORTE), and its variants.

2.2.1 The Even-Parity Formulation

The EPRTE is the first attempt that transforms the classic RTE into an equation with the second-order diffusion term and hence eliminates the convection-dominated property. The EPRTE was initially proposed in the field of neutron transport and has been used for decades. Song and Park (1992) initially applied the EPRTE in heat transfer field. It has been applied to DOM (Cheong and Song 1997) and FEM (Fiveland and Jessee 1995) discretization. In this approach, new variables, i.e., even- and odd-parity intensities, are defined as function of radiative intensity both at forward direction and backward direction,

$$\psi_{\mathrm{E}}(\mathbf{r},\boldsymbol{\Omega}) = \frac{1}{2}\left[I(\mathbf{r},\boldsymbol{\Omega}) + I\left(\mathbf{r},-\boldsymbol{\Omega}\right)\right] \tag{41}$$

$$\psi_{\mathrm{O}}(\mathbf{r},\boldsymbol{\Omega}) = \frac{1}{2}\left[I(\mathbf{r},\boldsymbol{\Omega}) - I\left(\mathbf{r},-\boldsymbol{\Omega}\right)\right] \tag{42}$$

By adding and subtracting the RTE (Eq. (12)) for forward direction $\boldsymbol{\Omega}$ and backward direction $-\boldsymbol{\Omega}$, respectively, it yields the governing equations of $\psi_{\mathrm{E}}(\mathbf{r}, \boldsymbol{\Omega})$ and $\psi_{\mathrm{O}}(\mathbf{r}, \boldsymbol{\Omega})$ for isotropic scattering media as

$$\boldsymbol{\Omega}\cdot\nabla\psi_{\mathrm{O}} + \beta\psi_{\mathrm{E}} = \kappa_a I_b + \frac{\kappa_s}{2\pi}\int_{2\pi}\psi_{\mathrm{E}}(\mathbf{r},\boldsymbol{\Omega}')\mathrm{d}\Omega' \tag{43}$$

$$\boldsymbol{\Omega}\cdot\nabla\psi_{\mathrm{E}} + \beta\psi_{\mathrm{O}} = 0 \tag{44}$$

These two equations can be decoupled. From Eq. (44), $\psi_{\mathrm{O}} = -\beta^{-1}\boldsymbol{\Omega}\cdot\nabla\psi_{\mathrm{E}}$, which is substituted into the first term of Eq. (43) to obtain a second-order diffusion-type equation of ψ_{E}, namely, the EPRTE,

$$-\boldsymbol{\Omega}\cdot\nabla\left(\beta^{-1}\boldsymbol{\Omega}\cdot\nabla\psi_{\mathrm{E}}\right) + \beta\psi_{\mathrm{E}} = \kappa_a I_b + \frac{\kappa_s}{2\pi}\int_{2\pi}\psi_{\mathrm{E}}(\mathbf{r},\boldsymbol{\Omega}')\mathrm{d}\Omega' \tag{45}$$

It is noted that the angular integration for the scattering term is only over half solid angular space. Since this is a second-order partial differential equation, boundary condition both at the inflow and outflow boundaries should be prescribed. Following similar approach, by adding and subtracting of the boundary condition (Eq.(36)) for forward direction $\boldsymbol{\Omega}$ and backward direction $-\boldsymbol{\Omega}$, the boundary condition for ψ_{E} at inflow ($\mathbf{n}_w\cdot\boldsymbol{\Omega} < 0$) and outflow ($\mathbf{n}_w\cdot\boldsymbol{\Omega} > 0$) boundary is obtained as

$$\begin{aligned}&\psi_{\mathrm{E}}(\mathbf{r}_w,\boldsymbol{\Omega}) - \beta^{-1}\boldsymbol{\Omega}\cdot\nabla\psi_{\mathrm{E}}\\ &= \varepsilon_w I_b(\mathbf{r}_w) + \frac{1-\varepsilon_w}{\pi}\int_{\mathbf{n}_w\cdot\boldsymbol{\Omega}'>0}\left[\psi_{\mathrm{E}}(\boldsymbol{\Omega},\mathbf{r}_w) + \beta^{-1}\boldsymbol{\Omega}\cdot\nabla\psi_{\mathrm{E}}\right]\left|\mathbf{n}_w\cdot\boldsymbol{\Omega}'\right| d\Omega'\end{aligned} \tag{46}$$

and

$$\begin{aligned}&\psi_{\mathrm{E}}(\mathbf{r}_w,\boldsymbol{\Omega})+\beta^{-1}\boldsymbol{\Omega}\cdot\nabla\psi_{\mathrm{E}}\\&=\varepsilon_w I_b(\mathbf{r}_w)+\frac{1-\varepsilon_w}{\pi}\int_{\mathbf{n}_w\cdot\boldsymbol{\Omega}'>0}\left[\psi_{\mathrm{E}}(\boldsymbol{\Omega},\mathbf{r}_w)-\beta^{-1}\boldsymbol{\Omega}\cdot\nabla\psi_{\mathrm{E}}\right]|\mathbf{n}_w\cdot\boldsymbol{\Omega}'|\,d\Omega'\end{aligned}\tag{47}$$

respectively.

2.2.2 The Second-Order RTEs

The SORTE (Zhao and Liu 2007a) and its variant (Zhao et al. 2013) proposed recently are diffusion-type equations similar to the heat conduction equation in anisotropic medium. Its governing variable is the radiative intensity, as compared to the EPRTE, of which the governing variable is the even parity of radiative intensity. These two approaches share similar stability due to the same basic underlying principle. The using of radiative intensity as solution variable is more convenient and easier to be applied to complex radiative transfer problems for the SORTEs, such as anisotropic scattering.

The SORTE is rather easy to be derived based on the RTE. From Eq. (7), it is rearranged to have

$$I=-\beta^{-1}\frac{\mathrm{d}I}{\mathrm{d}s}+(1-\omega)I_b+\frac{\omega}{4\pi}\int_{4\pi}I(s,\boldsymbol{\Omega}')\,\Phi(\boldsymbol{\Omega}'\cdot\boldsymbol{\Omega})d\Omega'\tag{48}$$

where $\omega=\kappa_s/\beta$ is the single scattering albedo. Substituting this relation back into the first term of the RTE, the SORTE is then obtained,

$$-\frac{\mathrm{d}}{\mathrm{d}s}\left[\beta^{-1}\frac{\mathrm{d}I}{\mathrm{d}s}\right]+\beta I=\beta S-\frac{\mathrm{d}S}{\mathrm{d}s}\tag{49}$$

where S is the source function defined as

$$S=(1-\omega)I_b+\frac{\omega}{4\pi}\int_{4\pi}I(\boldsymbol{\Omega}',s)\Phi(\boldsymbol{\Omega}'\cdot\boldsymbol{\Omega})d\Omega'$$

Following the approach in Sect. 2.1.2, the SORTE can be written in Cartesian coordinate as

$$-\boldsymbol{\Omega}\cdot\nabla\left[\beta^{-1}\boldsymbol{\Omega}\cdot\nabla I\right]+\beta I=\beta S-\boldsymbol{\Omega}\cdot\nabla S\tag{50}$$

and rewritten as

$$\nabla\cdot\left(\overline{\mathbf{K}}\cdot\nabla I\right)=\beta(I-S)+\boldsymbol{\Omega}\cdot\nabla S\tag{51}$$

where $\overline{\mathbf{K}}=\beta^{-1}\boldsymbol{\Omega}\boldsymbol{\Omega}$, which is similar to the tensorial heat conductivity for anisotropic medium, and the terms at the right-hand side can be viewed as effective heat source.

Similar to the EPRTE, the boundary condition for the SORTE should be prescribed both at the inflow and outflow boundaries. Since the governing variable is

radiative intensity, the boundary condition is straightforward, which is given at the inflow and outflow boundary as (Zhao and Liu 2007a)

$$I(\mathbf{r}_w, \mathbf{\Omega}) = \varepsilon_w I_b(\mathbf{r}_w) + \frac{1-\varepsilon_w}{\pi} \int_{\mathbf{n}_w \cdot \mathbf{\Omega}' > 0} I(\mathbf{r}_w, \mathbf{\Omega}') |\mathbf{n}_w \cdot \mathbf{\Omega}'| \, d\Omega', \quad \mathbf{n}_w \cdot \mathbf{\Omega} < 0 \tag{52}$$

$$\mathbf{\Omega} \cdot \nabla I(\mathbf{r}_w, \mathbf{\Omega}) + \beta I(\mathbf{r}_w, \mathbf{\Omega}) = \beta S(\mathbf{r}_w, \mathbf{\Omega}), \quad \mathbf{n}_w \cdot \mathbf{\Omega} > 0 \tag{53}$$

Note that the inflow boundary condition for SORTE is the same for that of the RTE and the outflow boundary condition is just the RTE itself.

Following the similar principle, the modified SORTE (MSORTE) was proposed (Zhao et al. 2013), in which no β^{-1} coefficient appears; hence, it is better in dealing with inhomogeneous media where some locations have very small/zero extinction coefficient. The MOSRTE is obtained by applying the stream operator d/ds once to the RTE, which can be written in ray-path coordinate as

$$\frac{\mathrm{d}^2 I}{\mathrm{d}s^2} + \frac{\mathrm{d}\beta I}{\mathrm{d}s} = \frac{\mathrm{d}\beta S}{\mathrm{d}s} \tag{54}$$

and in Cartesian coordinate system as

$$(\mathbf{\Omega} \cdot \nabla)^2 I + \mathbf{\Omega} \cdot \nabla(\beta I) = \mathbf{\Omega} \cdot \nabla(\beta S) \tag{55}$$

The boundary conditions for the MSORTE are the same as that for the SORTE.

2.2.3 Numerical Properties of the Second-Order RTE

The second-order form of RTE contains a second-order diffusion term, which circumvents the convection-dominated characteristics of the RTE, and hence is numerical stable. The numerical properties of the RTE, SORTE, and MSORTE have been studied theoretically using Fourier analysis (Zhao et al. 2013), which confirms the stability of the second-order forms of RTE. Figure 6 gives a comparison of the predicted relative solution error in frequency domain for the first-order and second-order form of RTEs. As can be seen, at high frequency ($\overline{\omega}$ closes to 0.5, which is the frequency of the unphysical oscillations), the relative error for the central difference discretization of the second-order form of RTEs is far less than (two orders of magnitude) that of the RTE, proving the numerical stability of the second-order form of RTEs.

2.3 The Radiative Transfer Equation in Refractive Media

Due to the structural characteristics of a material or a possible temperature, pressure, and composition dependency, the refractive index of a media may be a function of spatial position. In this case, the ray goes along a curved path determined by the Fermat principle rather than along the straight lines. The formulation of the RTEs

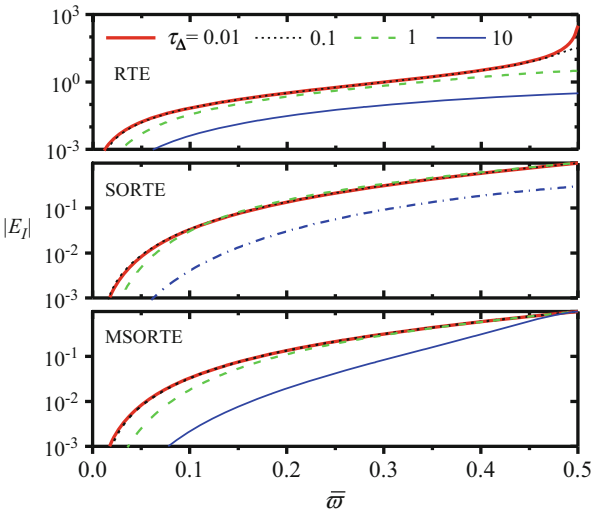

Fig. 6 The frequency domain distribution of solution error for the central difference discretization based on the RTE, the MSORTE, and the SORTE at different grid optical thickness (Zhao et al. 2013)

presented in the previous section implicitly assumed straight-line ray path. The effect of ray curvature or gradient index refraction has to be taken into account to formulate the radiative transfer equation in refractive media. Hence the RTE in uniform index media cannot be applied to gradient index media. The radiative heat transfer in semitransparent media with graded index is of significant importance in thermo-optical systems, atmospheric radiation, ocean optics, etc. and has evoked the wide interest of many researchers (Zhu et al. 2011; Asllanaj and Fumeron 2010; Sun and Li 2009; Liu 2006; Xia et al. 2002; Ben Abdallah and Le Dez 2000a, b). In this section, the radiative transfer equation in gradient refractive index media and its formulation under different coordinate system are presented.

2.3.1 Ray-Path Coordinate System Formulation

When a light beam propagates in gradient index media, its direction will gradually change due to the effect of gradient of refractive index, besides the attenuation and augmentation effect caused by absorption, scattering, and emission processes, as shown in Fig. 7. The governing equation of radiative transfer in gradient index media can be considered as an extension of the RTE to take into account the effect of gradient of refractive index.

The variation of radiative intensity along the curved ray path can be attributed to two mechanisms: the first is due to the variation of refractive index and the second is from any other processes as discussed in participating media of uniform refractive index distribution. The total variation of radiative intensity along the curved ray path can be written as

$$\mathrm{d}I_\lambda(s,n(s),\mathbf{s}) = \frac{\partial I_\lambda(s,n(s),\mathbf{s})}{\partial s}ds + \frac{\partial I_\lambda(s,n(s),\mathbf{s})}{\partial n}dn \tag{56}$$

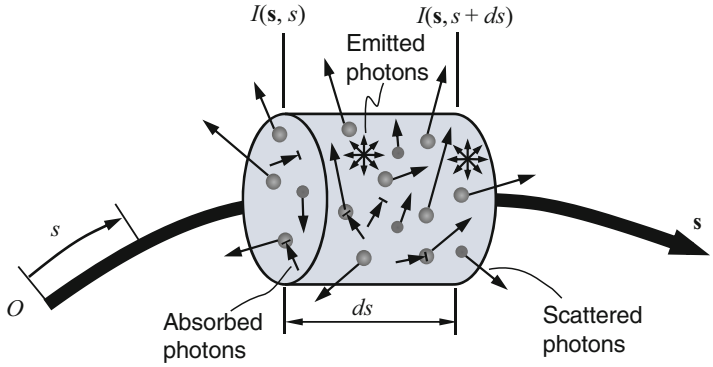

Fig. 7 Schematic of light transport in gradient index participating medium and variable definition in ray-path coordinate

where the first term on the right-hand side stands for the variation caused by the common processes of absorption, scattering, and emission, which can be expressed based on the RTE in uniform refractive index media as

$$\frac{\partial I_\lambda(s,n(s),\mathbf{s})}{\partial s} = -\beta_\lambda I_\lambda(\mathbf{s},s) \quad + \kappa_{a,\lambda} I_{b,\lambda}[T(s)] + \frac{\kappa_{s,\lambda}}{4\pi} \times \int_{4\pi} I_\lambda(s,\mathbf{\Omega}')\Phi_\lambda(\mathbf{\Omega}'\cdot\mathbf{s})\mathrm{d}\Omega' \tag{57}$$

The second term stands for the variation only caused by variation of refractive index, which is needed to be explicitly calculated. The Clausius invariant relation for transparent gradient index media gives $d[I_\lambda/n^2] = 0$, from which the second term in Eq. (56) can be obtained as

$$\frac{\partial I_\lambda}{\partial n} dn = 2\frac{I_\lambda}{n} dn \tag{58}$$

Substituting Eq. (58) into Eq. (56), then the radiative transfer equation in gradient index medium (GRTE) in Lagrange form along the ray coordinate can be obtained as

$$n^2 \frac{d}{ds}\left[\frac{I_\lambda(s,\mathbf{s})}{n^2}\right] + \beta_\lambda I_\lambda(\mathbf{s},s) \quad = \kappa_{a,\lambda} I_{b,\lambda}[T(s)] + \frac{\kappa_{s,\lambda}}{4\pi} \times \int_{4\pi} I_\lambda(s,\mathbf{\Omega}')\Phi_\lambda(\mathbf{\Omega}'\cdot\mathbf{s})\mathrm{d}\Omega' \tag{59}$$

By expanding the Lagrangian stream operator in Eulerian frame (Eq. (8)), the transient GRTE is obtained,

$$\frac{n_\lambda}{c}\frac{\partial I_\lambda(s,t,\mathbf{s})}{\partial t}+n^2\frac{\partial}{\partial s}\left[\frac{I_\lambda(s,t,\mathbf{s})}{n^2}\right]+\beta_\lambda I_\lambda(s,t,\mathbf{s}) = \kappa_{a,\lambda}I_{b,\lambda}[T(s)]+\frac{\kappa_{s,\lambda}}{4\pi}\int_{4\pi} I_\lambda(s,t,\mathbf{\Omega}')\Phi_\lambda(\mathbf{\Omega}'\cdot\mathbf{s})\mathrm{d}\Omega' \tag{60}$$

Note that the GRTE does not contain information about the curved ray path. To solve the equation, the ray equation (Born and Wolf 1970) must be solved, that is,

$$\frac{\mathrm{d}}{\mathrm{d}s}(n\mathbf{s})=\nabla n \tag{61}$$

The wavelength subscript will be omitted without loss of generality. More detailed derivation of radiative transfer equation in gradient refractive index media, including light polarization, refers to Ref. Zhao et al. 2012b.

2.3.2 Cartesian Coordinate System Formulation

To formulation the GRTE in Cartesian coordinate system, the stream operator needs to be explicitly expressed in this system. Assuming the radiative intensity is expressed as $I(\mathbf{r}, \mathbf{\Omega}) = I(x, y, z, \theta, \varphi)$, then the stream operator can be expanded as

$$\begin{aligned}\frac{d}{ds}&=\frac{dx}{ds}\frac{\partial}{\partial x}+\frac{dy}{ds}\frac{\partial}{\partial y}+\frac{dz}{ds}\frac{\partial}{\partial z}+\frac{d\theta}{ds}\frac{\partial}{\partial\theta}+\frac{d\varphi}{ds}\frac{\partial}{\partial\varphi}\\&=\mathbf{\Omega}\cdot\nabla+\frac{d\theta}{ds}\frac{\partial}{\partial\theta}+\frac{d\varphi}{ds}\frac{\partial}{\partial\varphi}\end{aligned} \tag{62}$$

To obtain the explicit formulation of the two angular derivatives, i.e., $d\theta/ds$ and $d\varphi/ds$, the ray equation (Eq. (61)) must be applied. Following the derivation in (Liu 2006), they can be written as

$$\frac{\mathrm{d}\varphi}{\mathrm{d}s}=\frac{1}{\sin\theta}\left(\mathbf{s}_1\cdot\frac{\nabla n}{n}\right),\quad \frac{\mathrm{d}\theta}{\mathrm{d}s}=\frac{1}{\sin\theta}\left[(\xi\mathbf{\Omega}-\mathbf{k})\cdot\frac{\nabla n}{n}\right] \tag{63}$$

where $\mathbf{s}_1$ is an auxiliary vector defined as $\mathbf{s}_1 = -\sin\varphi\mathbf{i}+\cos\varphi\mathbf{j}$. Substituting Eqs. (62) and (63) into the GRTE in ray coordinate (Eq.(59)) and after some manipulations, the final conservative form of the GRTE in Cartesian coordinate system can be obtained as

$$\begin{aligned}&\mathbf{\Omega}\cdot\nabla I(\mathbf{r},\mathbf{\Omega})+\frac{1}{\sin\theta}\frac{\partial}{\partial\theta}[I(\mathbf{r},\mathbf{\Omega})(\xi\mathbf{\Omega}-\mathbf{k})]\cdot\frac{\nabla n}{n}\\&+\frac{1}{\sin\theta}\frac{\partial}{\partial\varphi}[I(\mathbf{r},\mathbf{\Omega})\mathbf{s}_1]\cdot\frac{\nabla n}{n}+(\kappa_a+\kappa_s)I(\mathbf{r},\mathbf{\Omega})\\&=\kappa_a I_b(\mathbf{r})+\frac{\kappa_s}{4\pi}\int_{4\pi} I(\mathbf{r},\mathbf{\Omega}')\,\Phi(\mathbf{\Omega},\mathbf{\Omega}')\,d\Omega'\end{aligned} \tag{64}$$

The complete derivation refers to the work of Liu (2006). As compared to the RTE in Cartesian coordinate system (Eq. (12)), it is seen that there are two additional terms related to the gradient of refractive index (the second and third term) that appears in Eq. (64), which are also terms about derivatives of angular variable θ and φ and are usually called angular redistribution terms in literatures. It is angular redistribution terms that account for the effect of gradient refractive index distribution.

2.3.3 Formulation in Other Coordinate Systems

The formulation of GRTE in cylindrical and spherical coordinate system is presented here. Two types of the cylindrical coordinates system are considered as shown in Fig. 3. Following similar procedure outlined in Sect. 2.3.2, the GRTE in the Type I cylindrical coordinate system (ρ-Ψ-z-θ-φ) can be derived and written in conservative form as (Liu et al. 2006)

$$\begin{aligned}&\boldsymbol{\Omega}\cdot\widetilde{\nabla}_{\mathrm{I}}I-\frac{1}{\rho}\frac{\partial\eta I}{\partial\varphi}+\frac{1}{\sin\theta}\left\{\frac{\partial}{\partial\theta}\left[\left((\xi\boldsymbol{\Omega}-\mathbf{e}_z)\cdot\frac{\nabla n}{n}\right)I\right]+\frac{\partial}{\partial\varphi}\left[\left(\mathbf{s}_1\cdot\frac{\nabla n}{n}\right)I\right]\right\}\\&\quad+(\kappa_a+\kappa_s)I(\mathbf{r},\boldsymbol{\Omega})\\&\quad=\kappa_a I_b(\mathbf{r})+\frac{\kappa_s}{4\pi}\int_{4\pi}I(\mathbf{r},\boldsymbol{\Omega}')\,\Phi(\boldsymbol{\Omega},\boldsymbol{\Omega}')\,d\Omega'\end{aligned}\tag{65}$$

where $\boldsymbol{\Omega}=\mu\mathbf{e}_\rho+\eta\mathbf{e}_\Psi+\xi\mathbf{e}_z$ is the local direction vector of the beam; $\mu=\sin\theta\cos\varphi$; $\eta=\sin\theta\sin\varphi$; $\xi=\cos\theta$; $\mathbf{e}_\rho$, $\mathbf{e}_\Psi$ and $\mathbf{e}_z$ are the unit coordinate vector; $\widetilde{\nabla}_{\mathrm{I}}(\cdot)=\mathbf{e}_\rho\,\rho^{-1}\,\partial\,(\rho\,\cdot)/\,\partial\,\rho+\mathbf{e}_\Psi\rho^{-1}\,\partial\,(\cdot)/\,\partial\,\Psi+\mathbf{e}_z\rho^{-1}\,\partial\,(\cdot)/\,\partial\,z$ is a modified gradient operator in the Type I cylindrical coordinate system, and the auxiliary vector is defined as $\mathbf{s}_1=-\mathbf{e}_\rho\sin\varphi+\mathbf{e}_\Psi\cos\varphi$.

Similarly, the GRTE in the Type II cylindrical coordinate system (Ψ-z-ρ-θ-φ) can be obtained and written in conservative form as (Zhang et al. 2010; Zhao et al. 2012b)

$$\begin{aligned}&\boldsymbol{\Omega}\cdot\widetilde{\nabla}_{\mathrm{II}}I-\frac{1}{\rho\sin\theta}\frac{\partial}{\partial\theta}\left[\mu^2 I\right]+\frac{1}{\rho}\frac{\partial}{\partial\varphi}\left[\xi\sin\varphi\cos\varphi I\right]\\&\quad+\frac{1}{\sin\theta}\left\{\frac{\partial}{\partial\theta}\left[\left((\xi\boldsymbol{\Omega}-\mathbf{e}_z)\cdot\frac{\nabla n}{n}\right)I\right]+\frac{\partial}{\partial\varphi}\left[\left(\mathbf{s}_1\cdot\frac{\nabla n}{n}\right)I\right]\right\}\\&\quad+(\kappa_a+\kappa_s)I(\mathbf{r},\boldsymbol{\Omega})\\&\quad=\kappa_a I_b(\mathbf{r})+\frac{\kappa_s}{4\pi}\int_{4\pi}I(\mathbf{r},\boldsymbol{\Omega}')\,\Phi(\boldsymbol{\Omega},\boldsymbol{\Omega}')\,d\Omega'\end{aligned}\tag{66}$$

where $\boldsymbol{\Omega}=\mu\mathbf{e}_\Psi+\eta\mathbf{e}_z+\xi\mathbf{e}_\rho$ is the local direction vector of the beam, the auxiliary vector $\mathbf{s}_1=-\sin\varphi\mathbf{e}_\Psi+\cos\varphi\mathbf{e}_z$, and $\widetilde{\nabla}_{\mathrm{II}}(\cdot)=\mathbf{e}_\Psi\rho^{-1}\,\partial\,(\cdot)/\,\partial\,\Psi+\mathbf{e}_z\,\partial\,(\cdot)/\,\partial\,z+\mathbf{e}_\rho\rho^{-1}\,\partial\,(\rho\,\cdot)/\,\partial\,\rho$ is a modified gradient operator in the Type II cylindrical coordinate system.

The definition of the spherical coordinate system (Θ-Ψ-ρ-θ-φ) is shown in Fig. 4. Following the procedure outlined in Sect. 2.3.2, the GRTE in the spherical coordinate system can be obtained and written in conservative form as follows (Liu et al. 2006).

$$\begin{aligned}
&\boldsymbol{\Omega}\cdot\widetilde{\nabla} I-\frac{1}{\rho\sin\theta}\frac{\partial\sin^2\theta I}{\partial\theta}-\frac{\cot\Theta}{\rho}\frac{\partial\eta I}{\partial\varphi}\\
&+\frac{1}{\sin\theta}\left\{\frac{\partial}{\partial\theta}\left\{\left[\left(\xi\boldsymbol{\Omega}-\mathbf{e}_\rho\right)\cdot\frac{\nabla n}{n}\right]I\right\}+\frac{\partial}{\partial\varphi}\left[\left(\mathbf{s}_1\cdot\frac{\nabla n}{n}\right)I\right]\right\}\\
&+\ \ (\kappa_a+\kappa_s)I(\mathbf{r},\boldsymbol{\Omega})\\
&=\kappa_a I_b(\mathbf{r})+\frac{\kappa_s}{4\pi}\int_{4\pi} I(\mathbf{r},\boldsymbol{\Omega}')\,\Phi(\boldsymbol{\Omega},\boldsymbol{\Omega}')\,d\Omega'
\end{aligned}\tag{67}$$

where $\boldsymbol{\Omega}=\mu\mathbf{e}_\Theta+\eta\mathbf{e}_\Psi+\xi\mathbf{e}_\rho$ is the local direction vector of the beam, $\mathbf{s}_1=-\sin\varphi\mathbf{e}_\Theta+\cos\varphi\mathbf{e}_\Psi$ is an auxiliary vector the gradient operator, and $\widetilde{\nabla}$ is defined as $\widetilde{\nabla}(\cdot)=\mathbf{e}_\Theta(\rho\sin\Theta)^{-1}\,\partial\,(\sin\Theta\ \cdot)/\,\partial\,\Theta+\mathbf{e}_\Psi(\rho\sin\Theta)^{-1}\,\partial\,/\,\partial\,\Psi+\mathbf{e}_\rho\rho^{-2}\,\partial\,(\rho^2\cdot)/\,\partial\,\rho$.

3 Solution Techniques of the Radiative Transfer Equation

In this section, four fundamental deterministic methods for radiative transfer in participating media are introduced, including the spherical harmonics method, the DOM, FVM, and FEM. The spherical harmonics method is highly efficient for complex multidimensional problems. The DOM, FVM, and FEM are versatile, with good accuracy and convenient to be coupled with conduction and convection solvers. Note that several important aspects of numerical solution of radiative transfer equation are not covered in this chapter, such as the spectral models for non-gray media, problems with collimated irradiation, and transient radiative transfer.

3.1 Spherical Harmonics Method

Spherical harmonics method also known as P_N approximation is one basic type of method to solve radiative transfer. Especially, the lower-order approximations, such as P_1 and P_3 approximation, have achieved broad range of applications (Mengüç and Viskanta 1985; Mengüç and Iyer 1988). It is considered to suffer less from the ray effects, which can significantly deteriorate the accuracy of discrete-ordinate method. In the spherical harmonics method, the angular dependence of radiative intensity is expanded as a series of spherical harmonics, and the expansion coefficients are finally formulated into a set of partial differential equations to be solved. In this approach, the radiative intensity is approximated as

$$I(\mathbf{r},\mathbf{\Omega}) = \sum_{l=0}^{\infty} I_l^m(\mathbf{r}) Y_l^m(\mathbf{\Omega}) \tag{68}$$

where $Y_l^m(\mathbf{\Omega})$ are spherical harmonics, which are orthogonal functions in solid angular space, and $I_l^m(\mathbf{r})$ are the corresponding expansion coefficient. The governing equations for $I_l^m(\mathbf{r})$ can be obtained by substituting Eq. (68) into the RTE (Eq. (12)), and then do weighted angular integration with different orders of spherical harmonics.

It is usually very cumbersome to obtain the equations of $I_l^m(\mathbf{r})$, especially for higher-order approximation for multidimensional problems. Here, the P_1 approximation is presented. For the P_1 approximation, the expansion in Eq. (68) is truncated for $l > 1$. Four terms are retained in the series, and the radiative intensity can be shortly written as

$$I(\mathbf{r},\mathbf{\Omega}) = a(\mathbf{r}) + \mathbf{b}(\mathbf{r}) \cdot \mathbf{\Omega} \tag{69}$$

Substitute Eq. (69) into the RTE (Eq. (12)) to obtain

$$\begin{aligned} &\mathbf{\Omega} \cdot \nabla a(\mathbf{r}) + (\mathbf{\Omega}\mathbf{\Omega}) : \nabla \mathbf{b}(\mathbf{r}) + \beta[a(\mathbf{r}) + \mathbf{b}(\mathbf{r}) \cdot \mathbf{\Omega}] \\ &= \kappa_a I_b + \kappa_s a(\mathbf{r}) + \kappa_s g \mathbf{b}(\mathbf{r}) \cdot \mathbf{\Omega} \end{aligned} \tag{70}$$

Note that the last term is obtained using the following relation

$$\int_{4\pi} \mathbf{\Omega}' \Phi(\mathbf{\Omega}' \cdot \mathbf{\Omega}) \mathrm{d}\Omega' = \int_{4\pi} \begin{bmatrix} \sin\theta\cos\varphi \\ \sin\theta\sin\varphi \\ \cos\theta \end{bmatrix} \Phi(\cos\theta) \sin\theta d\theta d\varphi = 4\pi g \mathbf{\Omega} \tag{71}$$

where g is by definition the asymmetry factor of the scattering phase function. Equation (71) is in general not limited to the linear anisotropic scattering phase function. Integrate Eq. (70) for the zeroth and first moment to obtain the following two equations.

$$\nabla \cdot \mathbf{b}(\mathbf{r}) = 3\kappa_a [I_b - a(\mathbf{r})] \tag{72}$$

$$\mathbf{b}(\mathbf{r}) = -\frac{1}{\beta - \kappa_s g} \nabla a(\mathbf{r}) \tag{73}$$

The P_1 approximation equation can be obtained by substituting Eq. (73) into Eq. (72). The physical meaning of $a(\mathbf{r})$ and $\mathbf{b}(\mathbf{r})$ can be made clear by substituting Eq. (69) into the definition formula of radiative heat flux and incident radiation (Eq. (26)), which yields $a(\mathbf{r}) = \frac{G(\mathbf{r})}{4\pi}$ and $\mathbf{b}(\mathbf{r}) = \frac{3}{4\pi}\mathbf{q}$. Finally, the P_1 approximation equations are summarized below.

$$G \text{ equation}: \quad -\nabla \cdot \left[\frac{1}{3(\beta - \kappa_s g)} \nabla G\right] = \kappa_a (4\pi I_b - G) \tag{74}$$

$$q \text{ equation}: \qquad \mathbf{q} = -\frac{1}{3(\beta - \kappa_s g)}\nabla G \tag{75}$$

$$I \text{ equation}: \qquad I(\mathbf{r}, \mathbf{\Omega}) = \frac{1}{4\pi}[G(\mathbf{r}) + 3\mathbf{q}(\mathbf{r}) \cdot \mathbf{\Omega}] \tag{76}$$

By using the I equation, the boundary condition for diffuse emission and reflection boundary can be determined as

$$\frac{2-\varepsilon}{\varepsilon}\frac{2}{3(\beta - \kappa_s g)}\mathbf{n}_w \cdot \nabla G + G = 4\pi I_{bw} \tag{77}$$

At radiative equilibrium, namely, $\nabla \cdot \mathbf{q} = 0$ and $G = 4\pi I_b$, the q-equation (Eq. (75)) indicates

$$\mathbf{q} = -\frac{4\pi}{3(\beta - \kappa_s g)}\nabla I_b \tag{78}$$

This is the same as the Rosseland approximation (or diffusion approximation).

As can be seen, only one equation is needed to be solved (G equation) for radiative heat transfer; hence, it is highly efficient to be used to analyze engineering radiative transfer problems. Even though the P_1 approximation can give reasonable results for optically thick media, it may produce significant errors for optically thin media, in case the approximation Eq. (69) fails. The accuracy of P_1 approximation can be improved by using higher-order spherical harmonics, such as P_3 approximation. There are also a variant of P_N approximation, called the simplified P_N approximation (SP_N) (Larsen et al. 2002), which can generate equations consistent with P_1 approximation at low order and can be relatively easy to be extended to higher order.

3.2 Discrete-Ordinate Method

The discrete-ordinate method for the solution of radiative transfer was first proposed by Chandrasekhar (1960). It was then introduced to solve neutron transport, such as the work of Carlson and Lathrop (1965). Fiveland (1984) and Truelove (1988) applied the method to solve general radiative heat transfer problems. A recent review of the DOM and FVM was given by Coelho (2014). In the following, the basic principle of the method is presented. The solution of radiative transfer equation requires discretization of both angular and spatial domains. The idea of DOM is to represent the angular space by a discretized set of directions, and only radiative intensity at these discrete directions is solved. Each direction is associated with a quadrature weight. Both the directions and the weight are chosen carefully to ensure accuracy of angular integration, which is important for discretizing the in-scattering term and calculating the radiative heat flux. After the angular discretization is

finished, the original integral-differential form of RTE becomes a set of coupled partial differential equations, which can then be discretized and solved by traditional techniques for solving partial differential equations.

3.2.1 Angular Discretization

The angular space is discretized as a set of discrete directions, $\mathbf{\Omega}_m = \mu_m \mathbf{i} + \eta_m \mathbf{j} + \xi_m \mathbf{k}$; then the RTE (Eq. (12)) can be written into a set of partial differential equations, namely, the discrete-ordinate equations, as

$$\mathbf{\Omega}_m \cdot \nabla I_m(\mathbf{r}) + \beta I_m(\mathbf{r}) = \kappa_a I_b(\mathbf{r}) + \frac{\kappa_s}{4\pi} \sum_{m'=1}^{M} I_{m'}(\mathbf{r})\, \Phi(\mathbf{\Omega}_{m'} \cdot \mathbf{\Omega}_m)\, w_{m'}, \quad m = 1, \ldots, M \tag{79}$$

where w_m is the weight of direction $\mathbf{\Omega}_m$ for angular quadrature and M is the total number of discrete discretions. For the opaque and diffuse boundary, the boundary conditions for each discrete-ordinate equation are written as

$$I_w(\mathbf{\Omega}_m) = \varepsilon_w I_{bw} + \frac{1 - \varepsilon_w}{\pi} \sum_{\mathbf{n}_w \cdot \mathbf{\Omega}_{m'} > 0} I_w(\mathbf{\Omega}_{m'}) \left| \mathbf{n}_w \cdot \mathbf{\Omega}_{m'} \right| w_{m'}, \ \mathbf{\Omega}_m \cdot \mathbf{n}_w < 0 \tag{80}$$

By definition, the radiative heat flux and incident radiation are determined as

$$\mathbf{q}(\mathbf{r}) = \sum_{m=1}^{M} I^m(\mathbf{r}) \mathbf{\Omega}^m w^m, \ \ G(\mathbf{r}) = \sum_{m=1}^{M} I^m(\mathbf{r})\, w^m \tag{81}$$

The definition of the angular discretization includes the selection of the set discrete directions (ordinates) and the design of the related angular quadrature, which is critical about the accuracy of the method. There are several criteria proposed on the selection of angular discretization and the weights (Fiveland 1984; Carlson and Lathrop 1965): (1) The symmetry criterion, namely, the discrete set of directions and weights, should be the same after the rotation of $\pi/2$ about each principle axis (x-,y- and z-). (2) The full space moment preserving criterion, i.e., the angular quadrature defined based on the selected directions, should satisfy the zeroth, first, and second moments integrated over 4π, namely,

$$\int_{4\pi} d\Omega = 4\pi = \sum_{m=1}^{M} w^m \tag{82}$$

$$\int_{4\pi} \mathbf{\Omega} d\Omega = \mathbf{0} = \sum_{m=1}^{M} \mathbf{\Omega}^m w^m \tag{83}$$

$$\int_{4\pi} \mathbf{\Omega}\mathbf{\Omega} d\Omega = \frac{4\pi}{3}\boldsymbol{\delta} = \sum_{m=1}^{M} \mathbf{\Omega}^m \mathbf{\Omega}^m w^m \tag{84}$$

where $\mathbf{0}$ denotes the zero vector and $\boldsymbol{\delta}$ is the unit tensor. (3) The half space moment preserving criterion, i.e., the defined angular quadrature, should preserve the first moment integration over 2π, requiring

$$\begin{aligned} \int_{\mu>0} \mu d\Omega = \pi = \sum_{\mu_m>0} \mu_m w_m \\ \int_{\eta>0} \eta d\Omega = \pi = \sum_{\eta_m>0} \eta_m w_m \\ \int_{\xi>0} \xi d\Omega = \pi = \sum_{\xi_m>0} \xi_m w_m \end{aligned} \tag{85}$$

The most well-known family of the discrete-ordinate set is the S_N sets, initially proposed for simulation of neutron transport (Carlson and Lathrop 1965), which are also tabulated in the classic textbooks (Howell et al. 2011; Modest 2013). The angular discretization using the S_N discrete-ordinate set is usually called S_N-approximation. For the S_N-approximation, such as S_2, S_4, or S_6, N means the number of discrete direction cosines used for each principal direction. Total number of directions for the S_N-approximation is $M = N(N + 2)$. Several other discrete-ordinate sets were also proposed, such as the T_N sets by Thurgood et al. (1995). A recent review of the angular discretization schemes in DOM was given by Koch and Becker (2004).

3.2.2 Spatial Discretization

After angular discretization, the resulting discrete-ordinate equations (Eq. (79)) for each direction $\mathbf{\Omega}^m$ can then be discretized by common methods for solving partial differential equations, such as finite difference method and FVM. Note that upwinding scheme is required to obtain reliable results considering the numerical property of the RTE discussed in Sect. 2.1.6; an alternative is to use the second-order form of RTE for discretization.

Here, the FVM is used to discretize Eq. (79) to obtain the final algebraic equation. The advantage of FVM is that it is easy to be applied to unstructured mesh to solve problems with complex geometry. Figure 8 shows the 2D grid used to define the FVM discretization scheme. The unknown radiative intensities are stored at the center of each grid cell. By integrating Eq. (79) over the control volume P and using the Gaussian divergence theorem to the first term, it yields

$$\Delta x\left(\mu_m I_{m,\ e} - \mu_m I_{m,\ w}\right) + \Delta y\left(\eta_m I_{m,\ n} - \eta_m I_{m,\ s}\right) + \beta_P I_{m,P} \Delta x \Delta y = S_{m,P} \Delta x \Delta y \tag{86}$$

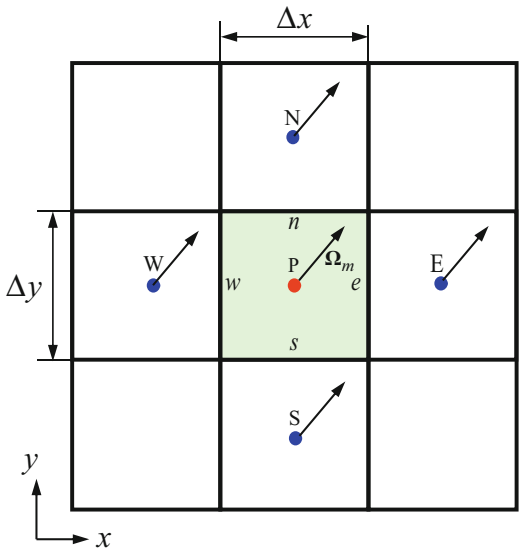

Fig. 8 Grid used to define the FVM discretization

where the subscript of capitalized letters denotes the value at cell center (P) and subscript of small letters (e, w, n and s) denotes values at the center of faces as shown in Fig. 8; $S_{m,P}$ is the source term defined as

$$S_{m,P} = S_m(\mathbf{r}_P) = \kappa_a I_b(\mathbf{r}_P) + \frac{\kappa_s}{4\pi}\sum_{m'=1}^{M} I_{m'}(\mathbf{r}_P)\,\Phi(\boldsymbol{\Omega}_{m'}\cdot\boldsymbol{\Omega}_m)\,w_{m'} \tag{87}$$

Since radiative intensities are stored at cell center only, interpolation of radiative intensity at faces to that at cell center is required to obtain the final algebraic equations. Using interpolation and supposing uniform grid, the face values can be interpolated using neighboring cell values as

$$I_{m,n} = \alpha_y I_{m,P} + \big(1-\alpha_y\big)I_{m,N}, I_{m,e} = \alpha_x I_{m,P} + (1-\alpha_x)I_{m,E} \tag{88a}$$

$$I_{m,s} = \alpha_y I_{m,S} + \big(1-\alpha_y\big)I_{m,P}, I_{m,w} = \alpha_x I_{m,W} + (1-\alpha_x)I_{m,P} \tag{88b}$$

where α_x and α_y are the interpolation parameters for x and y directions, respectively. Substituting Eq. (88) into Eq. (86), the final discretization can be written as

$$a_P I_{m,P} = a_N I_{m,N} + a_S I_{m,S} + a_W I_{m,W} + a_E I_{m,E} + b \tag{89}$$

where the discrete coefficients are determined as

$$\begin{aligned} &a_N = \eta_m \Delta y\big(\alpha_y - 1\big),\quad a_E = \mu_m \Delta x(\alpha_x - 1),\quad a_S = \eta_m \Delta y \alpha_y,\quad a_W = \mu_m \Delta x \alpha_x \\ &a_P = a_N + a_S + a_W + a_E + \beta_P \Delta x \Delta y,\quad b = S_{m,P}\Delta x \Delta y \end{aligned} \tag{90}$$

Different differencing schemes can be obtained by defining different interpolation parameters, such as (1) step scheme (or first-order upwind scheme), $\alpha_x = \text{unitstep}(\mu_m)$ and $\alpha_y = \text{unitstep}(\eta_m)$, and (2) diamond scheme (or central difference scheme), $\alpha_x = \alpha_y = 1/2$.

The resulting linear systems in Eq. (89) can be solved element by element until the convergence, which can also be solved by sparse solvers. Since the source term contains radiative intensity of other directions, a global iteration is required to successively update the source terms for problems with scattering media and reflecting boundary conditions. The discretization presented above can be easily extended to 3D problems. The extension to unstructured mesh is presented in the next section.

3.3 Finite Volume Method

Raithby and Chui (Chui and Raithby 1992; Raithby and Chui 1990) firstly formulated FVM for solving radiative heat transfer problems. Chai and coworkers (Chai and Lee 1994; Chai et al. 1993) developed different variant implementation of FVM. A comprehensive review of the development of DOM and FVM was given recently by Coelho (2014). In the FVM method, both the angular domain and the spatial domain are discretized by using control volume integration. The angular discretization in FVM is thus different from the DOM. The angular domain discretization in FVM uses structured mesh as shown in Fig. 9, while the spatial domain can be structured or unstructured. Though different from DOM, the FVM can be formulated in a very similar fashion with DOM. As such the major difference between DOM and FVM lies in the angular discretization.

3.3.1 Angular Discretization

Integrate the RTE (Eq. (12)) over a small control angle of Ω^{ml} centered at direction $\mathbf{\Omega}^{ml}$ (the superscript m and l denotes the index of θ and φ discretization, respectively), and assuming the radiative intensity is constant in Ω^{ml}, it leads to

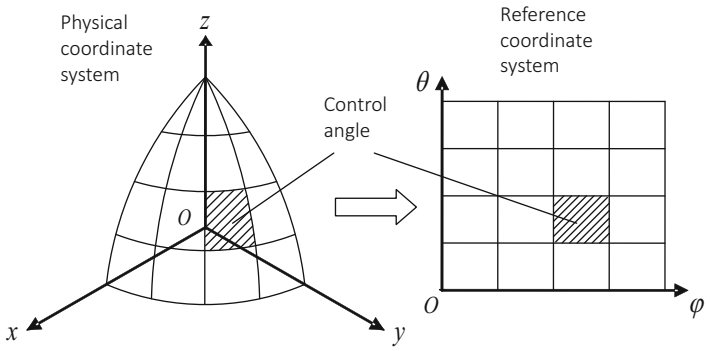

Fig. 9 Schematic of angular grid used in FVM discretization

$$\int_{\Omega^{ml}} \mathbf{\Omega} d\Omega \cdot \nabla I^{ml}(\mathbf{r}) + \beta \ \Omega^{ml} I^{ml}(\mathbf{r}) = \Omega^{ml} S^{ml}(\mathbf{r}) \tag{91}$$

where $S^{ml}(\mathbf{r})$ is given as

$$S^{ml}(\mathbf{r}) = \kappa_a I_b(\mathbf{r}) + \frac{\kappa_s}{4\pi} \sum_{l'=1}^{N_\varphi} \sum_{m'=1}^{N_\theta} I^{m'l'}(\mathbf{r}) \overline{\Phi}\left(\mathbf{\Omega}^{m'l'} \cdot \mathbf{\Omega}^{ml}\right) \Omega^{m'l'} \tag{92}$$

in which $\overline{\Phi}\left(\mathbf{\Omega}^{m'l'} \cdot \mathbf{\Omega}^{ml}\right) = \frac{1}{\Omega^{m'l'}\Omega^{ml}} \int_{\Omega^{ml}} \int_{\Omega^{m'l'}} \Phi\left(\mathbf{\Omega}^{m'l'} \cdot \mathbf{\Omega}^{ml}\right) d\Omega' \ d\Omega.$

Dividing Ω^{ml} to both sides of Eq. (91), an equation in the form of discrete-ordinate equation (Eq. (79)) is obtained, which is written as

$$\overline{\mathbf{\Omega}}^{ml} \cdot \nabla I^{ml}(\mathbf{r}) + \beta \ I^{ml}(\mathbf{r}) = S^{ml}(\mathbf{r}) \tag{93}$$

where $\overline{\mathbf{\Omega}}^{ml}$ is an averaged direction vector defined as

$$\overline{\mathbf{\Omega}}^{ml} = \frac{1}{\Omega^{ml}} \int_{\Omega^{ml}} \mathbf{\Omega} d\Omega \tag{94}$$

Note that $\overline{\mathbf{\Omega}}^{ml}$ can be calculated analytically (Murthy and Mathur 1998). Taking $\overline{\mathbf{\Omega}}^{ml}$ as the equivalent discrete direction in DOM, the quantities, such as heat flux, incident radiation, etc., can be calculated the same way as in the DOM.

3.3.2 Spatial Discretization

Since mathematical form of Eq. (93) is the same as the discrete-ordinate equation, the spatial FVM discretization procedure described in the previous section for DOM can be directly applied. Here only formulation on unstructured mesh is introduced, which can also be applied to the DOM for spatial discretization instability. Considering the unknowns are stored in the center of the control volume cell, integrating Eq. (93) over a spatial control volume and applying the Gaussian divergence theorem to the first term leads to

$$\sum_{i=1}^{N_f} A_{f_i} I_{f_i}^{ml} \overline{\mathbf{\Omega}}^{ml} \cdot \mathbf{n}_{f_i} + \beta_P I_P^{ml} \Delta V_P = S_P^{ml} \Delta V_P \tag{95}$$

where the subscript f_i denotes value at the i-th face of control volume centered at P, the subscript P denotes value at point P, $\mathbf{n}$ is the surface normal, A is area of the face, and ΔV_P is the volume of the control volume centered at P. To complete the

discretization, the intensity defined at surface should be interpolated to nodal values (volume center), which can be generally written as

$$I_{f_i}^{ml} = \alpha_i I_P^{ml} + (1 - \alpha_i) I_{P_i}^{ml} \tag{96a}$$

where P_i denotes the center of the neighboring cell of i-th face of the cell P. With this closure relation, the final FVM discretization can be written as

$$a_P I_P^{ml} = \sum_{i=1}^{N_f} a_{P_i} I_{P_i}^{ml} + b^{ml} \tag{97}$$

where the discrete coefficients are given as

$$\begin{aligned} a_P &= \sum_{i=1}^{N_f} A_{f_i} \alpha_i \overline{\mathbf{\Omega}}^{ml} \cdot \mathbf{n}_{f_i} + \beta_P \Delta V_P \\ a_{P_i} &= A_{f_i} (\alpha_i - 1) \overline{\mathbf{\Omega}}^{ml} \cdot \mathbf{n}_{f_i} \\ b^{ml} &= S_P^{ml} \Delta V_P \end{aligned} \tag{98}$$

If the step scheme (or first-order upwind) is used, then $\alpha_i = \text{unitstep}\left(\overline{\mathbf{\Omega}}^{ml} \cdot \mathbf{n}_{f_i}\right)$. Equation (97) for each control angle can be solved element by element and iterates until convergence.

3.4 Finite Element Method

Fiveland and Jesse (1994) were the first to apply the FEM to solve radiative heat transfer problems based on the differential form of RTE. Until recently, many variant implementations of FEM have been proposed (Liu 2004b; W. An et al. 2005; Zhao and Liu 2007a; Zhang et al. 2016). After angular discretization, as described in Sects. 3.2 and 3.3, the RTE becomes a set of partial differential equations, i.e., the discrete-ordinate equations, which can then be solved by common numerical method for solving partial differential equations. Similar to FVM, FEM is another versatile method that can be applied to solve a broad range of partial differential equations that appeared in scientific and engineering problems and hence is very appealing for multiphysics simulation. The feature of FEM is that it usually owns higher order of accuracy as compared to the FVM. In the FEM, the unknown radiative intensity is first approximated as a series of shape functions, which is then combined with the weighted residual approach to discretize the RTE; finally a sparse linear system is obtained and solved by general solvers. Here the FEM for solving the RTE is introduced.

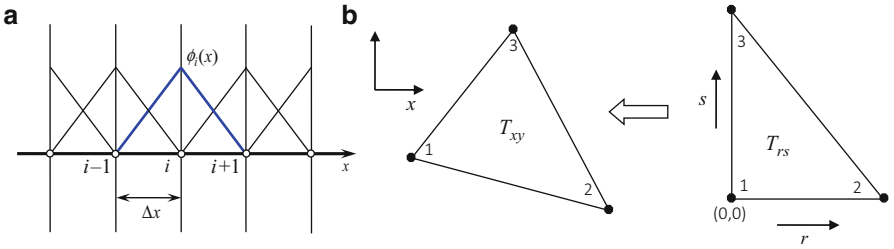

Fig. 10 (**a**) Schematic of nodal shape function of 1D linear elements in FEM. (**b**) Transform of linear elements defined on reference space to physical space

3.4.1 Function Approximation

The solid angular space discretization is by common the discrete-ordinate approach, such as the S_N sets or the FVM approach described in Sects. 3.2 and 3.3. The radiative intensity for each discrete direction $\mathbf{\Omega}_m$ can be approximated using the FEM shape functions ϕ_i at each solution nodes, namely,

$$\tilde{I}_m(\mathbf{x}) \simeq \sum_{i=1}^{N_{sol}} I_{m,i}\phi_i(\mathbf{x}) \tag{99}$$

where $I_{m,i}$ are the expansion coefficients, which are also the values of the radiative intensity of direction $\mathbf{\Omega}_m$ at node i (namely, $I_{m,i} = I(\mathbf{\Omega}_m,\mathbf{x}_i)$) due to the Kronecker delta property of the FEM shape functions. For example, the global shape function at node i for the 1D linear element can be written as

$$\phi_i(x) = \begin{cases} (x - x_{i-1})/\Delta x, & x_{i-1} \le x < x_i \\ (x_{i+1} - x)/\Delta x, & x_i \le x < x_{i+1} \\ 0, & \text{otherwise} \end{cases}, \tag{100}$$

which is also graphically shown in Fig. 10a for better understanding.

Generally, for multidimensional complex elements, the shape function on an element can be first defined in a reference space, and then transformed to the physical space, as shown in Fig. 10b, where a linear triangular element is taken as an example. For 2D triangular element, the three shape functions defined in reference space (r-t) can be written as

$$\Gamma_1(r,s) = 1 - r - s, \;\; \Gamma_2(r,s) = r, \;\; \Gamma_3(r,s) = s \tag{101}$$

which can be transformed to obtain the shape function in physical space (x-y) as

$$\phi_i(x(r,s), y(r,s)) = \Gamma_i(r,s), \;\; i = 1,2,3 \tag{102}$$

The coordinate system transformation from reference element T_{rs}: {(0, 0), (1, 0), (0, 1)} to physical element T_{xy}:{$(\hat{x}_1,\hat{y}_1), (\hat{x}_2,\hat{y}_2), (\hat{x}_3,\hat{y}_3)$} is defined as

$$x = \sum_{i=1}^{3} \hat{x}_i \Gamma_i(r,s), \qquad y = \sum_{i=1}^{3} \hat{y}_i \Gamma_i(r,s) \tag{103}$$

where $\hat{x}_i, \hat{y}_i$, $i = 1, 2, 3$ denote the coordinates of the nodes that define the triangular element.

3.4.2 Weighted Residual Approach

The discrete-ordinate equation (Eq. (79)) can be written as

$$\mathbf{\Omega}_m \cdot \nabla I_m(\mathbf{r}) + \beta I_m(\mathbf{r}) = S_m(\mathbf{r}) \tag{104}$$

where the source term $S(\mathbf{r}, \mathbf{\Omega})$ is defined as

$$S_m(\mathbf{r}) = \kappa_a I_b(\mathbf{r}) + \frac{\kappa_s}{4\pi} \sum_{m'=1}^{M} I_{m'}(\mathbf{r})\, \Phi(\mathbf{\Omega}_{m'} \cdot \mathbf{\Omega}_m)\, w_{m'} \tag{105}$$

Using weighted residual approach, Eq. (104) is weighted by a set of weight functions $W_j(\mathbf{r})$ and integrated over the solution domain, which leads to (Liu et al. 2008)

$$\left\langle \mathbf{\Omega}_m \cdot \nabla I_m(\mathbf{r}), W_j(\mathbf{r}) \right\rangle + \left\langle \beta I_m(\mathbf{r}), W_j(\mathbf{r}) \right\rangle = \left\langle S_m(\mathbf{r}), W_j(\mathbf{r}) \right\rangle \tag{106}$$

where the inner product $< \cdot \ , \ \cdot >$ is defined as $< f, g >= \int_V fg \mathrm{d}V$.

By substituting the approximated radiative intensity (Eq. (99)) into weighted residual approach equation (Eq. (106)) and choosing different set of weight functions, a discrete set of linear equations can be obtained, which can be written in matrix form as

$$\mathbf{K}_m \mathbf{u}_m = \mathbf{h}_m \tag{107}$$

where $\mathbf{u}_m = \left[u_{m,i}\right]_{i=1,N_{sol}} = \left[I_m(\mathbf{r}_i)\right]_{i=1,N_{sol}}$, $\mathbf{K}_m$, and $\mathbf{h}_m$ are conventionally called stiff matrix and load vector, respectively, which are different for different FEM discretization. The selection of the weighted function results in different FEM discretization schemes, such as for Galerkin scheme (Galerkin FEM), which chooses $W_j = \phi_j$, and for least-squares scheme (LSFEM) to choose $W_j = \mathbf{\Omega}_m \cdot \nabla \phi_j + \beta \phi_j$. Note that the LSFEM formulation can also be derived based on functional minimization procedure.

For the Galerkin FEM discretization, $\mathbf{K}_m$ and $\mathbf{h}_m$ are obtained as (Liu et al. 2008)

$$\mathbf{K}_m = \left[K_{m,ji}\right]_{j=1,N_{sol};i=1,N_{sol}} = \ < \mathbf{\Omega}_m \cdot \nabla \phi_i, \phi_j > + < \beta \phi_i, \phi_j > \tag{108a}$$

$$\mathbf{h}_m = \left[h_{m,j}\right]_{j=1,N_{sol}} =< S_m, \phi_j > \tag{108b}$$

For the LSFEM discretization, $\mathbf{K}_m$ and $\mathbf{h}_m$ are obtained as (Zhao et al. 2012a)

$$\mathbf{K}_m = \left[K_{m,ji}\right]_{j=1,N_{sol};\ i=1,N_{sol}}$$

$$=< \boldsymbol{\Omega}_m \cdot \nabla\phi_i, \boldsymbol{\Omega}_m \cdot \nabla\phi_j > + < \beta\phi_i, \beta\phi_j > \tag{109a}$$

$$+ < \beta\phi_i, \boldsymbol{\Omega}_m \cdot \nabla\phi_j > + < \boldsymbol{\Omega}_m \cdot \nabla\phi_i, \beta\phi_j >$$

$$\mathbf{h}_m = \left[h_{m,j}\right]_{j=1,N_{sol}} =< S_m, \beta\phi_j > + < S_m, \boldsymbol{\Omega}_m \cdot \nabla\phi_j > \tag{109b}$$

It is noted that the stiff matrix produced by LSFEM is symmetric and positive definite, which is a very good numerical property.

The accuracy in the imposing of this type of boundary condition is very important for the overall solution accuracy. One accurate method for imposing the Dirichlet-type boundary condition is operator collocation approach. In this approach, the row of stiff matrix $\mathbf{K}_m$ corresponding to the inflow boundary nodes is replaced with the discrete operator of the related boundary condition. Similar modification is also applied to the load vector $\mathbf{h}_m$. The modification algorithm is formulated as below (the modification is only conducted for nodes on the inflow boundary, namely, $\mathbf{n}_w(\mathbf{r}_j) \cdot \boldsymbol{\Omega}_m < 0$).

$$K_{m,ji} = \delta_{ji}, \tag{110a}$$

$$h_{m,j} = I_0\left(\mathbf{r}_j, \boldsymbol{\Omega}_m\right) \tag{110b}$$

where $I_0(\mathbf{r}_j, \boldsymbol{\Omega}_m)$ stands for the radiative intensity at the boundary given by Eq. (80).

The FEM has also been successfully applied to the second-order form of RTEs to avoid the stability problem caused by the convection-dominated property of the first-order RTE, and this kind of FEM has been demonstrated to be numerically stable and accurate (Fiveland and Jessee 1994; Zhao and Liu 2007a; Zhang et al. 2016).

3.5 Solution Methods for RTE in Refractive Media

Many numerical methods have been developed for the solution of radiative transfer in gradient index media, which include the curved ray-tracing-based methods (Ben Abdallah and Le Dez 2000b; Ben Abdallah et al. 2001; Huang et al. 2002a, b; Liu 2004a; Wang et al. 2011) and the methods based on discretization of the GRTE. The ray tracing is usually cumbersome and time consuming in calculation. Lemonier and Le Dez (Lemonnier and Le Dez 2002) pioneered the discrete-ordinate method for solving the GRTE. Their work is for one-dimensional problem. Thereafter, Liu (2006) formulated the discrete-ordinate equation of GRTE for general multi-dimensional problems, which forms the basis for the solution of radiative transfer in gradient index media. It is like the role of discrete-ordinate equation of RTE in uniform index media. Based on the discrete-ordinate equation, the spatial

discretization techniques, such as FVM and FEM, can be readily applied for solution. Besides the FEM and FVM, many other numerical methods have been developed to solve radiative heat transfer in gradient index media based on the discrete-ordinate equation of GRTE (Zhao and Liu 2007b; Sun and Li 2009; Asllanaj and Fumeron 2010; Zhang et al. 2015).

In this section, only the solution techniques based on the discretization of the GRTE is introduced. Generally, the basic principle to solve the GRTE is the same as that for radiative transfer in uniform index media. As outlined in previous sections, the first is to discretize the angular space to transform the integral-differential equation into a set of partial differential equations, namely, the discrete-ordinate equations. The second step is to spatially discretize the discrete-ordinate equations, which can be done by common methods such as finite difference, FVM and FEM, etc. However, the GRTE differs from the RTE in uniform index media for containing two angular redistribution terms, which have derivatives with respect to angular variables. The discrete-ordinate equation of GRTE is the key for different solution methods. However, to determine the discrete-ordinate equations for GRTE is not so straightforward as that for the RTE (Lemonnier and Le Dez 2002; Liu 2006).

In the following, the discrete-ordinate equations for GRTE are presented. The detailed derivation refers to Liu (2006) Liu and Tan (2006). Formally, the discrete-ordinate equations of GRTE can be written as

$$\begin{aligned}
&\boldsymbol{\Omega}^{m,n}\cdot\nabla I(\mathbf{r},\boldsymbol{\Omega}^{m,n})+\left[\frac{1}{\sin\theta}\frac{\partial}{\partial\theta}\left\{I(\mathbf{r},\boldsymbol{\Omega})(\xi\boldsymbol{\Omega}-\mathbf{k})\right\}\right]_{\Omega=\Omega^{m,n}}\cdot\frac{\nabla n}{n}\\
&+\left[\frac{1}{\sin\theta}\frac{\partial}{\partial\varphi}\left(I(\mathbf{r},\boldsymbol{\Omega})\,\mathbf{s}_1\right)\right]_{\Omega=\Omega^{m,n}}\cdot\frac{\nabla n}{n}+(\kappa_a+\kappa_s)I(\mathbf{r},\boldsymbol{\Omega}^{m,n})\\
&=\kappa_a I_b+\frac{\kappa_s}{4\pi}\sum_{m'=1}^{N_\theta}\sum_{n'=1}^{N_\varphi}I\left(\mathbf{r},\boldsymbol{\Omega}^{m',n'}\right)\Phi\left(\boldsymbol{\Omega}^{m',n'},\boldsymbol{\Omega}^{m,n}\right)w_\theta^{m'}w_\varphi^{n'}
\end{aligned}\tag{111}$$

where piecewise constant angular quadrature (PCA) is used to discrete the angular space, in which the total solid angle is divided uniformly in the polar θ and azimuthal φ directions, defined as

$$\theta^m=(m-1/2)\Delta\theta,\quad m=1,\cdots,N_\theta \tag{112a}$$

$$\varphi^n=(n-1/2)\Delta\varphi,\quad n=1,\cdots,N_\varphi \tag{112b}$$

where $\Delta\theta=\pi/N_\theta$ and $\Delta\varphi=2\pi/N_\varphi$ are steps for the discretization of polar and azimuthal angles, respectively, and N_θ and N_φ are the corresponding number of divisions. For each discrete direction (m,n), the corresponding weight is

$$w_\theta^m=\cos\theta^{m-1/2}-\cos\theta^{m+1/2},\quad w_\varphi^n=\varphi^{n+1/2}-\varphi^{n-1/2}, \tag{113}$$

where $\theta^{m+1/2}=(\theta^m+\theta^{m+1})/2$, $\varphi^{n+1/2}=(\varphi^n+\varphi^{n+1})/2$.

The two angular redistribution terms can be formally discretized as

$$\left[\frac{1}{\sin\theta}\frac{\partial}{\partial\theta}\{I(\xi\mathbf{\Omega}-\mathbf{k})\}\cdot\frac{\nabla n}{n}\right]_{\Omega=\Omega^{m,n}} \simeq \frac{\chi_\theta^{m+1/2,n} I^{m+1/2,n} - \chi_\theta^{m-1/2,n} I^{m-1/2,n}}{w_\theta^m}, \tag{114a}$$

$$\left[\frac{1}{\sin\theta}\frac{\partial}{\partial\varphi}(I(\mathbf{r},\Omega)\mathbf{s}_1)\cdot\frac{\nabla n}{n}\right]_{\Omega=\Omega^{m,n}} \simeq \frac{\chi_\varphi^{m,n+1/2} I^{m,n+1/2} - \chi_\varphi^{m,n-1/2} I^{m,n-1/2}}{w_\varphi^n}. \tag{114b}$$

Details on determining the discrete coefficients of χ_θ and χ_φ were presented in Ref. Liu (2006). Substitute Eq. (114) into Eq. (64) and apply necessary closure relations (Liu 2006). The final discrete-ordinate equation of GRTE can be obtained and expressed in a form similar to the discrete-ordinate equation of RTE, i.e.,

$$\mathbf{\Omega}^{m,n}\cdot\nabla I^{m,n} + \tilde{\beta}^{m,n}(\mathbf{r}) I^{m,n} = \tilde{S}^{m,n}(\mathbf{r}), \tag{115a}$$

where the modified extinction coefficient $\tilde{\beta}^{m,n}(\mathbf{r})$ and modified source term $\tilde{S}^{m,n}(\mathbf{r})$

$$\begin{aligned}\tilde{\beta}^{m,n}(\mathbf{r}) = {} & \frac{1}{w_\theta^m}\max\left(\chi_\theta^{m+1/2,n},0\right) + \frac{1}{w_\theta^m}\max\left(-\chi_\theta^{m-1/2,n},0\right) \\ & + \frac{1}{w_\varphi^n}\max\left(\chi_\varphi^{m,n+1/2},0\right) + \frac{1}{w_\varphi^n}\max\left(-\chi_\varphi^{m,n-1/2},0\right) + (\kappa_a+\kappa_s)\end{aligned} \tag{115a}$$

$$\begin{aligned}\tilde{S}^{m,n}(\mathbf{r}) = {} & n^2\kappa_a I_b + \frac{\kappa_s}{4\pi}\sum_{m'=1}^{N_\theta}\sum_{n'=1}^{N_\varphi} I^{m',n'}\Phi^{m',n';m,n} w_\theta^{m'} w_\varphi^{n'} \\ & + \frac{1}{w_\theta^m}\max\left(-\chi_\theta^{m+1/2,n},0\right) I^{m+1,n} \\ & + \frac{1}{w_\theta^m}\max\left(\chi_\theta^{m-1/2,n},0\right) I^{m-1,n} \\ & + \frac{1}{w_\varphi^n}\max\left(-\chi_\varphi^{m,n+1/2},0\right) I^{m,n+1} \\ & + \frac{1}{w_\varphi^n}\max\left(\chi_\varphi^{m,n-1/2},0\right) I^{m,n-1}\end{aligned} \tag{115b}$$

The recursion formula for $\chi_\theta^{m+1/2,n}$ and $\chi_\varphi^{m,n+1/2}$ is given below.

$$\chi_\theta^{m+1/2,n} - \chi_\theta^{m-1/2,n} = \frac{w_\theta^m}{\sin\theta^m}\left[\frac{\partial(\xi\mathbf{\Omega})}{\partial\theta}\cdot\frac{\nabla n}{n}\right]_{\Omega=\Omega^{m,n}} \tag{116a}$$

$$\chi_\theta^{1/2,n} = \chi_\theta^{N_\theta+1/2,n} = 0 \tag{116b}$$

$$\chi_{\varphi}^{m,\,n+1/2} - \chi_{\varphi}^{m,\,n-1/2} = \frac{w_{\varphi}^{n}}{\sin\theta^{m}} \left[\frac{\partial \mathbf{s}_1}{\partial \varphi} \cdot \frac{\nabla n}{n} \right]_{\Omega=\Omega^{m,\,n}} \tag{116c}$$

$$\chi_{\varphi}^{m,\,1/2} = \chi_{\varphi}^{m,\,N_{\varphi}+1/2} = \frac{1}{\sin\theta^{m}} \left(\mathbf{j} \cdot \frac{\nabla n}{n} \right) \tag{116d}$$

Similar to the discrete-ordinate equations of RTE, Eq. (115) with boundary conditions is solved for each discrete direction. Since both $\tilde{\beta}^{m,\,n}(\mathbf{r})$ and $\tilde{S}^{m,\,n}(\mathbf{r})$ contain part of angular redistribution terms, it is different from the discrete-ordinate equation of RTE. The source term updating is always needed during the solution process. The spatial discretization techniques, such as FVM and FEM presented in the previous sections, can be readily applied to Eq. (115) for solution. Note that the discretization of the GRTE can also be conducted without relying on the discrete-ordinate equation. Recently, Zhang et al. (2012) developed a hybrid FEM/FVM technique to solve the GRTE, in which the angular domain is discretized using FEM and spatial domain is discretized using FVM, and the radiative intensity at all the directions is solved simultaneously at each spatial node. The idea of this approach follows the work of Coelho (2005) for solving the RTE.

4 Numerical Errors and Accuracy Improvement Strategies

All numerical methods suffer from numerical errors. The MC method suffers from statistic errors, while the DOM, FVM, and FEM suffer from space and angular discretization errors. Due to the significant importance in real applications, numerical errors for solving RTE have attracted the interest of many researchers (Chai et al. 1993; Ramankutty and Crosbie 1997; Coelho 2002b; Hunter and Guo 2015; Huang et al. 2011; Tagne Kamdem 2015). In this section, DOM is taken as an example method, and the numerical errors that appear in DOM and the related improvement strategies are discussed.

4.1 Origin of Numerical Errors in DOM

The "false scattering" and "ray effects" are terms to describe the characteristics of the numerical error observed in numerical results of DOM. Literally, "false scattering" means the effect of the numerical error behave like scattering process, which was usually considered to be equivalent to numerical diffusion (Chai et al. 1993). The "ray effects" stand for the unphysical bump that appeared in the numerical results, which was attributed to using of discrete number of directions to approximate the continuous angular variation of radiative intensity (Chai et al. 1993).

In order to understand the origin of the error phenomenon, it is necessary to analyze the source of errors in DOM. By carefully checking the DOM discretization of RTE and the calculation of heat flux and incident radiation, three major sources of

errors can be identified: (1) error from differencing scheme, which is related to the discretization of a differential operator in spatial domain; (2) error from the discretization of scattering term, which is related to the discretization of an integral operator in angular domain; and (3) error from the calculation of heat flux or incident radiation, which is related to the discretization of another integral operator. Note that the third source is distinctly different from the second source, since it will appear even if the medium is non-scattering. What is the effect of these three sources of errors? What is the relation of these three sources of errors with "false scattering" and "ray effects," which will be discussed in the following section?

4.2 Error from Differencing Scheme

A differencing scheme is required to discretize the differential operator in the discrete-ordinate equation of RTE (Eq. (79)). Take step scheme as an example, which is equivalent to the first-order upwind finite difference scheme. Assuming $\mu_m > 0$, it can be discretized for the x-direction as

$$\mu_m \frac{\partial I_m}{\partial x} \simeq \mu_m \frac{I_m(x) - I_m(x - \Delta x)}{\Delta x} \tag{117}$$

Using Taylor expansion, the right-hand side of the above discretization can be written as

$$\mu_m \frac{I_m(x) - I_m(x - \Delta x)}{\Delta x} = \mu_m \frac{\partial I_m}{\partial x} + \left[\frac{1}{2}\mu_m \Delta x\right] \frac{\partial^2 I_m}{\partial x^2} + O\left(\Delta x^2\right) \tag{118}$$

As seen, an additional diffusion term appears (the second-order term), which has a diffusion coefficient of $\mu_m \Delta x/2$. Namely, the dominant error for step scheme is a diffusion process. This numerical diffusion will smooth the radiative intensity distribution, making additional radiative heat flux transport from high-intensity region to low-intensity region, similar to the heat conduction process. It is of significant difference from the scattering process, such as it only smears radiative flux of one direction, while the scattering process usually transfers energy from one direction to another direction. As such, this error is preferable to be called numerical diffusion. Hunter and Guo (2015) derived the expression of numerical diffusion of several differencing schemes, including the step scheme, diamond scheme, and QUICK scheme. The numerical diffusion can be significantly reduced if a high-order scheme is applied. For a low-order scheme like the step scheme, the numerical diffusion will decrease with mesh refinement.

Figure 11a shows the solved heat flux by DOM with step scheme at coarse grid (15×15) and fine grid (125×125), in which the data are extracted from the work by Coelho (2002b). The angular discretization is extremely fine; hence, the effect of angular discretization error can be neglected, and only the effect of numerical diffusion is observed. At coarse grid, big numerical diffusion appears, and the heat flux value is always greater than the exact value, which agrees with the analysis presented above.

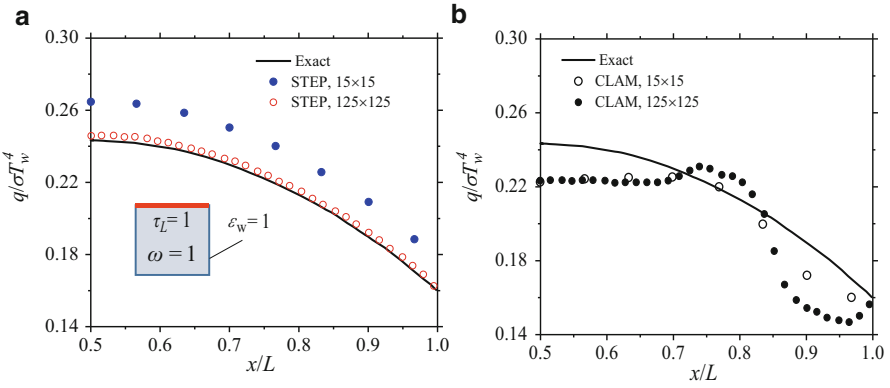

Fig. 11 Incident heat flux along the bottom wall to illustrate numerical diffusion and ray effects. (**a**) Step scheme, $N_\theta = N_\varphi = 100$ per octant, (**b**) CLAM scheme, S_8 approximation is used. Data are exacted from Coelho (2002b). Insets show the shape of enclosure; the top wall is hot and others are cold

4.3 Scattering Term Discretization Error

The DOM approximates the in-scattering term as

$$\int_{4\pi} I(\mathbf{\Omega}', \mathbf{r})\Phi(\mathbf{\Omega}' \cdot \mathbf{\Omega})\mathrm{d}\Omega' \simeq \sum_{m'=1}^{M} I_{m'}(\mathbf{r}_P)\,\Phi^{m'm} w_{m'} \tag{119}$$

This approximation will inevitably introduce discretization errors. Since the scattering phase function and radiative intensity distribution are usually complicated, this angular quadrature may introduce significant errors for scattering media, e.g., the phase function with strong forward peak. The discretization error of this term is considered to alter the contribution of original scattering phase function. By this understanding, this error induces unphysical scattering, i.e., false scattering, which changes the coupling of radiative intensity among different directions unphysically.

To improve the discretization accuracy of scattering phase function, several techniques have been proposed. The first is to modify the discrete phase function to ensure the exact energy conservation constraint, i.e.,

$$\sum_{m'=1}^{M} \Phi^{m'm} w_{m'} = 4\pi \tag{120}$$

The most common approach is to modify the phase function as follows (Liu et al. 2002):

$$\widetilde{\Phi}^{m'm} = \Phi^{m'm}\left(\frac{1}{4\pi}\sum_{m'=1}^{M} \Phi^{m'm} w_{m'}\right)^{-1} \tag{121}$$

which will ensure $\widetilde{\Phi}^{m'm}$ exactly satisfy the energy conservation relation.

Hunter and Guo (2012a, 2012b) showed that the normalization given in Eq. (121) is not enough for strongly forward-scattering phase function, e.g., asymmetry factor greater than 0.9. In this case, another constraint on conservation of asymmetry factor g should also be satisfied for the modified scattering phase function to get reliable results, namely,

$$\sum_{m'=1}^{M} \Phi^{m'm} w_{m'} \cos\left(\Theta^{m'm}\right) = 4\pi g \tag{122}$$

They then devised new schemes to normalize the discrete scattering phase function to ensure both the conservation of energy (Eq. (120)) and the conservation of asymmetry factor be satisfied (Hunter and Guo 2012a, 2014). Detailed normalization procedure refers to the pioneer work of Hunter and Guo (2012a). A recent work on comparison of the different normalization schemes for strongly forward-scattering phase function was given by Granate et al. (2016). The errors that arise from discretization of the scattering term was also called "angular false scattering" in Ref. Hunter and Guo (2015).

4.4 Error from Heat Flux Calculation

The phenomenon of ray effects is that the heat flux distribution contains unphysical bump pattern of errors, as shown in Fig. 11b. It mainly influences the solution accuracy of DOM when there are sharp gradients or discontinuities in the boundary conditions, temperature distribution, or radiative properties of the medium. Ray effects have been demonstrated to mainly rely on angular discretization (Lathrop 1968; Chai et al. 1993). Figure 11b shows the heat flux distribution along the bottom wall solved by CLAM scheme at a course (15 × 15) and fine (125 × 125) spatial grid; S_8 approximation is used for angular quadrature. It is known that CLAM scheme is a second-order accurate and bounded non-oscillatory scheme. However, even for the fine grid that spatial discretization is considered to be sufficiently accurate, there are still strong unphysical bump patterns in the heat flux distribution. Hence the numerical error featured with the bump pattern is unrelated with the spatial discretization. Furthermore, this kind of bump patterns contained in heat flux distribution still exists for the media without scattering (Coelho 2002b). Hence it cannot be attributed to the error from the scattering term. It has a distinct origin.

Here the bump pattern of numerical error is attributed to the inaccurate heat flux calculation. Figure 12a shows a typical configuration that has strong ray effects. In this case, only a confined load is located at the bottom, and the heat flux distribution along the top wall is to be calculated. Considering the media is non-scattering, the incident radiative intensity at the top wall can be traced back to the load. Point O denotes the center of the top wall and B is a point located with a distance from the center. The blue and red lines start from O, and B indicates the discrete-ordinate

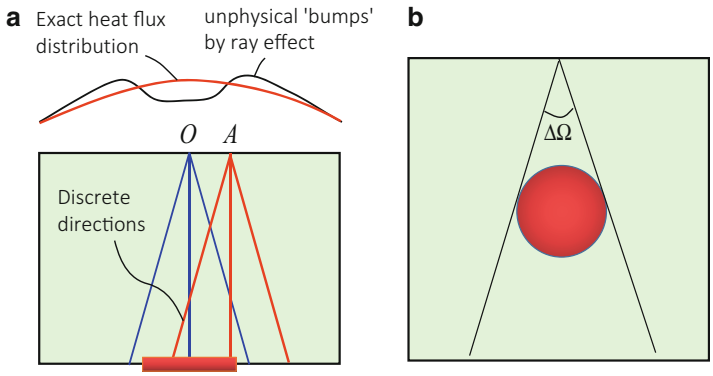

Fig. 12 Schematics to illustrate ray effects. (**a**) Boundary confined load, (**b**) inside (volumetric) confined load

directions, which are traced back to determine the intensities exactly. As can be seen, for point B, there are two directions intercepted with the load. As for the center point O, only one direction intercepts with the load. If angular quadrature is used to calculate the heat flux, it is obvious that heat flux at point B will be greater than that at the center point. This analysis agrees with the numerical results. Besides the confined boundary load, confined volumetric load (as shown in Fig. 12b) will also induce ray effects as studied by Coelho (2002b, 2004). The confinement of radiative intensity in a small solid angle is difficult to be accurately integrated, because only few discrete-ordinate directions will be located in the small solid angle to do integration. The ray effects can be mitigated by refining the angular discretization (Chai et al. 1993; Li et al. 2003); however, this approach requires considerable computational effort. It can also be effectively mitigated by the modified discrete-ordinate approach (Ramankutty and Crosbie 1997; Coelho 2002b; Coelho 2004), which treats the contributions from boundary load and volumetric load to heat flux separately by solving a different transfer equation. Recently, several new approaches were proposed to mitigate the ray effects in FVM and DOM. More effective way to mitigate the ray effects in DOM is still an important subject of research (Huang et al. 2011; Tagne Kamdem 2015).

5 Conclusions

In this chapter, the classical radiative transfer equation and several variant forms of radiative transfer equation, the different solution techniques for the radiative transfer equations, and the numerical errors on the solution of radiative transfer equation and the related improvement strategies are presented and discussed. The classical RTE implies the light propagates through straight line. To analyze radiative transfer in gradient index media where light propagates through curved lines, the GRTE should be applied. Under Cartesian coordinate the GRTE contains two terms of angular

derivatives as compared to the RTE, which account for the effect of gradient refractive index. The classical RTE is in a form of a first-order integral partial differential equation. It can be considered as a special kind of convection-diffusion equation with convection-dominated property. This is also true for the GRTE. The convection-dominated property will induce numerical instability for numerical solution. The classical RTE can be transformed to second-order forms and avoids the stability problem.

Numerical methods to solve radiative transfer can be classified into two groups, (1) methods based on stochastic simulation and (2) the deterministic methods, which are usually formulated based on the integral or differential form of RTE. The MCM is a typical method of the first group; it is versatile and reliable, but usually time consuming since a huge number of photons need to be traced and are inconvenient to be coupled with conduction and convection solvers; the latter are usually implemented using deterministic methods such as FVM and FEM. DOM is the typical method of the second group. The FVM can be considered as a special kind of DOM that the discrete-ordinate equations are obtained based on the FVM. FEM is usually more accurate than the FVM; furthermore, it is very versatile and promising for the simulation of multiphysics processes including radiative heat transfer.

Three major sources of errors for numerical solution of RTE can be identified: (1) error from differencing scheme, which is related to the discretization of a differential operator; (2) error from the discretization of scattering term, which is related to the discretization of an angular integral operator; and (3) error from the calculation of heat flux or incident radiation, which is related to the discretization of another angular integral operator. The first will induce numerical diffusion, in which radiative energy diffuses to the same direction. The second will induce unphysically altered phase function and hence is the true "false scattering." The third will induce unphysical bump pattern of errors in the flux distribution, also known as "ray effects," which is attributed to inaccuracy of angular quadrature. But this is distinctly different from the second source, since it will appear even if the medium is non-scattering. Besides the errors mentioned above, it should be noted that the actual solution accuracy of radiative transfer problems also relies closely on the accuracy of measured material properties, such as absorption coefficient, scattering coefficient, and scattering phase function, which should be cared for the solution of real problems.

6 Cross-References

- ▶ A Prelude to the Fundamentals and Applications of Radiation Transfer
- ▶ Monte Carlo Methods for Radiative Transfer
- ▶ Radiative Plasma Heat Transfer
- ▶ Radiative Properties of Gases
- ▶ Radiative Properties of Particles
- ▶ Radiative Transfer in Combustion Systems

Acknowledgements The authors thank the supports by National Nature Science Foundation of China (Nos. 51336002, 51421063). The support by the Fundamental Research Funds for the Central Universities (Grant No. HIT. NSRIF. 2013094, HIT.BRETIII.201415) are also greatly acknowledged.

References

Agrafiotis CC, Mavroidis I, Konstandopoulos AG, Hoffschmidt B, Stobbe P, Romero M, Fernandez-Quero V (2007) Evaluation of porous silicon carbide monolithic honeycombs as volumetric receivers/collectors of concentrated solar radiation. Sol Energy Mater Sol Cells 91(6):474–488

An W, Ruan LM, Qi H, Liu LH (2005) Finite element method for radiative heat transfer in absorbing and anisotropic scattering media. J Quant Spectrosc Radiat Transf 96(3–4):409–422

Asllanaj F, Fumeron S (2010) Modified finite volume method applied to radiative transfer in 2D complex geometries and graded index media. J Quant Spectrosc Radiat Transf 111(2):274–279

Ben Abdallah P, Le Dez V (2000a) Thermal emission of a semi-transparent slab with variable spatial refractive index. J Quant Spectrosc Radiat Transf 67(3):185–198

Ben Abdallah P, Le Dez V (2000b) Thermal field inside an absorbing-emitting semitransparent slab at radiative equilibrium with variable spatial refractive index. J Quant Spectrosc Radiat Transf 65(4):595–608

Ben Abdallah P, Charette A, Le Dez V (2001) Influence of a spatial variation of the thermo-optical constants on the radiative transfer inside an absorbing–emitting semi-transparent sphere. J Quant Spectrosc Radiat Transf 70(3):341–365

Benoit H, Spreafico L, Gauthier D, Flamant G (2016) Review of heat transfer fluids in tube-receivers used in concentrating solar thermal systems: properties and heat transfer coefficients. Renew Sust Energ Rev 55:298–315

Berberoglu H, Yin J, Pilon L (2007) Light transfer in bubble sparged photobioreactors for H2 production and CO2 mitigation. J Quant Spectrosc Radiat Transf 32(13):2273–2285

Born M, Wolf E (1970) Principles of optics, 7th edn. Cambridge University Press, Cambridge

Carlson BG, Lathrop KD (1965) Transport theory: the method of discrete ordinates. In: Greenspan H, Kelber CN, Okrent D (eds) Computational methods in reactor physics. Gordon and Breach, New York, pp 171–270

Chai JC, Lee HS (1994) Finite-volume method for radiation heat transfer. J Thermophys Heat Transf 8(32):419–425

Chai JC, Lee HO, Patankar SV (1993) Ray effect and false scattering in the discrete ordinates method. Numer Heat Transf B 24(4):373–389

Chai JC, Lee HS, Patankar SV (2000a) Finite-volume method for radiation heat transfer. Adv Numer Heat Transf 2:109–141

Chai JC, Lee HS, Patankar SV (2000b) Finite-volume method for radiation heat transfer. In: Minkowycz WJ, Sparrow EM (eds) Advances in numerical heat transfer, vol 2. Taylor & Francis, New York, pp 109–141

Chai JL, Cheng Q, Song JL, Wang ZC, Zhou HC (2015) The DRESOR method for one-dimensional transient radiative transfer in graded index medium coupled with BRDF surface. Int J Therm Sci 91:96–104

Chandrasekhar S (1960) Radiative transfer. Dover Publications, New York

Cheong KB, Song TH (1997) An alternative discrete ordinates method with interpolation and source differencing for two-dimensional radiative transfer problems. Numer Heat Transf B 32(1):107–125

Chui EH, Raithby GD (1992) Implicit solution scheme to improve convergence rate in radiative transfer problems. Numer Heat Transf B 22(3):251–272

Coelho PJ (2002a) Bounded skew high-order resolution schemes for the discrete ordinates method. J Comput Phys 175(2):412–437

Coelho PJ (2002b) The role of ray effects and false scattering on the accuracy of the standard and modified discrete ordinates methods. J Quant Spectrosc Radiat Transf 73:231–238
Coelho PJ (2004) A modified version of the discrete ordinates method for radiative heat transfer modelling. Comput Mech 33(5):375–388
Coelho PJ (2005) A hybrid finite volume/finite element discretization method for the solution of the solution of the radiative heat transfer equation. J Quant Spectrosc Radiat Transf 93(1–3):89–101
Coelho PJ (2014) Advances in the discrete ordinates and finite volume methods for the solution of radiative heat transfer problems in participating media. J Quant Spectrosc Radiat Transf 145:121–146
Farmer JT, Howell JR (1994) Monte Carlo prediction of radiative heat transfer in inhomogeneous, anisotropic, nongray media. J Thermophys Heat Transf 8(1):133–139
Fiveland WA (1984) Discrete-ordinates solution of the radiative transport equation for rectangular enclosures. J Heat Transf 106(4):699–706
Fiveland WA (1988) Three-dimensional radiative heat-transfer solutions by the discrete-ordinates method. J Thermophys Heat Transf 2(4):309–316
Fiveland WA, Jessee JP (1994) Finite element formulation of the discrete-ordinates method for multidimensional geometries. J Thermophys Heat Transf 8(3):426–433
Fiveland WA, Jessee JP (1995) Comparison of discrete ordinates formulations for radiative heat transfer in multidimensional geometries. J Thermophys Heat Transf 9(1):47–54
Granate P, Coelho PJ, Roger M (2016) Radiative heat transfer in strongly forward scattering media using the discrete ordinates method. J Quant Spectrosc Radiat Transf 172:110–120
Hou M-F, Wu C-Y, Hong Y-B (2015) A closed-form solution of differential approximation for radiative transfer in a planar refractive medium. Int J Heat Mass Transf 83:229–234
Howell JR (1968) Application of Monte Carlo to heat transfer problems. Adv Heat Transf 5:1–54
Howell JR, Siegel R, Menguc MP (2011) Thermal radiation heat transfer, 5th edn. CRC Press, New York
Huang Y, Xia XL, Tan HP (2002a) Radiative intensity solution and thermal emission analysis of a semitransparent medium layer with a sinusoidal refractive index. J Quant Spectrosc Radiat Transf 74(2):217–233
Huang Y, Xia XL, Tan HP (2002b) Temperature field of radiative equilibrium in a semitransparent slab with a linear refractive index and gray walls. J Quant Spectrosc Radiat Transf 74(2):249–261
Huang ZF, Zhou HC, Hsu P (2011) Improved discrete ordinates method for ray effects mitigation. J Heat Transf 133(4):044502
Huang Y, Shi G-D, Zhu K-Y (2016) Runge–Kutta ray tracing technique for solving radiative heat transfer in a two-dimensional graded-index medium. J Quant Spectrosc Radiat Transf 176:24–33
Hunter B, Guo Z (2012a) Conservation of asymmetry factor in phase function discretization for radiative transfer analysis in anisotropic scattering media. Int J Heat Mass Transf 55(5):1544–1552
Hunter B, Guo Z (2012b) Phase-function normalization in the 3-D discrete-ordinates solution of radiative transfer – part II: benchmark comparisons. Numer Heat Transf B 62(4):223–242
Hunter B, Guo Z (2014) A new and simple technique to normalize the HG phase function for conserving scattered energy and asymmetry factor. Numer Heat Transf B 65(3):195–217
Hunter B, Guo Z (2015) Numerical smearing, ray effect, and angular false scattering in radiation transfer computation. Int J Heat Mass Transf 81:63–74
Klose AD, Netz U, Beuthan J, Hielscher AH (2002) Optical tomography using the time-independent equation of radiative transfer – part 1: forward model. J Quant Spectrosc Radiat Transf 72(5):691–713
Koch R, Becker R (2004) Evaluation of quadrature schemes for the discrete ordinates method. J Quant Spectrosc Radiat Transf 84(4):423–435
Larsen EW, Thommes G, Klar A, Seaid M, Gotz T (2002) Simplified PN approximations to the equations of radiative heat transfer and applications. J Comput Phys 183(2):652–675

Lathrop KD (1968) Ray effects in discrete ordinates equations. Nucl Sci Eng 32:357–369
Lemonnier D, Le Dez V (2002) Discrete ordinates solution of radiative transfer across a slab with variable refractive index. J Quant Spectrosc Radiat Transf 73(2–5):195–204
Li H-S, Flamant G, Lu J-D (2003) Mitigation of ray effects in the discrete ordinates method. Numer Heat Transf B 43(5):445–466
Li B-W, Sun Y-S, Yu Y (2008) Iterative and direct Chebyshev collocation spectral methods for one-dimensional radiative heat transfer. Int J Heat Mass Transf 51(25–26):5887–5894
Liou KN (2002) An introduction to atmospheric radiation. Academic press
Liu LH (2004a) Discrete curved ray-tracing method for radiative transfer in an absorbing-emitting semitransparent slab with variable spatial refractive index. J Quant Spectrosc Radiat Transf 83 (2):223–228
Liu LH (2004b) Finite element simulation of radiative heat transfer in absorbing and scattering media. J Thermophys Heat Transf 18(4):555–557
Liu LH (2006) Finite volume method for radiation heat transfer in graded index medium. J Thermophys Heat Transf 20(1):59–66
Liu LH, Tan HP (2006) Numerical simulation of radiative transfer in graded index media. Science Press, Beijing
Liu LH, Tan JY (2007) Least-squares collocation meshless approach for radiative heat transfer in absorbing and scattering media. J Quant Spectrosc Radiat Transf 103(3):545–557
Liu LH, Ruan LM, Tan HP (2002) On the discrete ordinates method for radiative heat transfer in anisotropically scattering media. Int J Heat Mass Transf 45(15):3259–3262
Liu LH, Zhang L, Tan HP (2006) Radiative transfer equation for graded index medium in cylindrical and spherical coordinate systems. J Quant Spectrosc Radiat Transf 97(3):446–456
Liu LH, Zhao JM, Tan HP (2008) The finite element method and spectral element method for numerical simulation of radiative transfer equation. Science Press, Beijing
Mahian O, Kianifar A, Kalogirou SA, Pop I, Wongwises S (2013) A review of the applications of nanofluids in solar energy. Int J Heat Mass Transf 57(2):582–594
Maruyama S (1993) Radiation heat transfer between arbitrary three-dimensional bodies with specular and diffuse surfaces. Numer Heat Transf A Appl 24(2):181–196
Mengüç MP, Iyer RK (1988) Modeling of radiative transfer using multiple spherical harmonics approximations. J Quant Spectrosc Radiat Transf 39(6):445–461
Mengüç MP, Viskanta R (1985) Radiative transfer in three-dimensional rectangular enclosures containing inhomogeneous, anisotropically scattering media. J Quant Spectrosc Radiat Transf 33(6):533–549
Modest MF (2013) Radiative heat transfer, 3rd edn. Academic Press, New York
Modest MF, Haworth DC (2016) Radiative heat transfer in turbulent combustion systems: theory and applications. Springer International Publishing, Cham
Murthy JY, Mathur SR (1998) Finite volume method for radiative heat transfer using unstructured meshes. J Thermophys Heat Transf 12(3):313–321
Pilon L, Berberoglu H, Kandilian R (2011) Radiation transfer in photobiological carbon dioxide fixation and fuel production by microalgae. J Quant Spectrosc Radiat Transf 112(17):2639–2660
Raithby GD, Chui EH (1990) A finite-volume method for predicting a radiant heat transfer in enclosures with participating media. J Heat Transf 112:415–423
Ramankutty MA, Crosbie AL (1997) Modified discrete ordinates solution of radiative transfer in two-dimensional rectangular enclosures. J Quant Spectrosc Radiat Transf 57(11):107–140
Sadat H (2006) On the use of a meshless method for solving radiative transfer with the discrete ordinates formulations. J Quant Spectrosc Radiat Transf 101(2):263–268
Siegel R, Howell JR (2002) Thermal radiation heat transfer, 4th edn. Taylor & Francis, New York
Simmons FS (2000) Rocket exhaust plume phenomenology. Aerospace Corporation
Song TH, Park CW 1992 Formulation and application of the second-order discrete ordinate method. In: Wang B-X (ed) Transport phenomena and science. Higher Education Press, Beijing, pp 833–841
Sun Y-S, Li B-W (2009) Chebyshev collocation spectral method for one-dimensional radiative heat transfer in graded index media. Int J Therm Sci 48:691–698

Tagne Kamdem HT (2015) Ray effects elimination in discrete ordinates and finite volume methods. J Thermophys Heat Transf 29(2):306–318

Thurgood CP, Pollard A, Becker HA (1995) The TN quadrature set for the discrete ordinates method. J Heat Transf 117(4):1068–1070

Truelove JS (1988) Three-dimensional radiation in absorbing-emitting-scattering media using discrete-ordinate approximation. J Quant Spectrosc Radiat Transf 39(1):27–31

Viskanta R, Mengüç MP (1987) Radiation heat transfer in combustion systems. Prog Energy Combust Sci 13(2):97–160

Wang Z, Cheng Q, Wang G, Zhou H (2011) The DRESOR method for radiative heat transfer in a one-dimensional medium with variable refractive index. J Quant Spectrosc Radiat Transf 112(18):2835–2845

Wu C-Y, Hou M-F (2012) Solution of integral equations of intensity moments for radiative transfer in an anisotropically scattering medium with a linear refractive index. Int J Heat Mass Transf 55 (7–8):1863–1872

Xia XL, Huang Y, Tan HP (2002) Thermal emission and volumetric absorption of a graded index semitransparent medium layer. J Quant Spectrosc Radiat Transf 74(2):235–248

Zhang L, Zhao JM, Liu LH (2010) Finite element approach for radiative transfer in multi-layer graded index cylindrical medium with Fresnel surfaces. J Quant Spectrosc Radiat Transf 111(3):420–432

Zhang L, Zhao JM, Liu LH, Wang SY (2012) Hybrid finite volume/finite element method for radiative heat transfer in graded index media. J Quant Spectrosc Radiat Transf 113(14):1826–1835

Zhang Y, Yi H-L, Tan H-P (2015) Analysis of transient radiative transfer in two-dimensional scattering graded index medium with diffuse energy pulse irradiation. Int J Therm Sci 87:187–198

Zhang L, Zhao JM, Liu LH (2016) A new stabilized finite element formulation for solving radiative transfer equation. J Heat Transf 138(6):064502–064502

Zhao JM, Liu LH (2006) Least-squares spectral element method for radiative heat transfer in semitransparent media. Numer Heat Transf B 50(5):473–489

Zhao JM, Liu LH (2007a) Second order radiative transfer equation and its properties of numerical solution using finite element method. Numer Heat Transf B 51:391–409

Zhao JM, Liu LH (2007b) Solution of radiative heat transfer in graded index media by Least Square spectral element method. Int J Heat Mass Transf 50:2634–2642

Zhao JM, Tan JY, Liu LH (2012a) A deficiency problem of the least squares finite element method for solving radiative transfer in strongly inhomogeneous media. J Quant Spectrosc Radiat Transf 113(12):1488–1502

Zhao JM, Tan JY, Liu LH (2012b) On the derivation of vector radiative transfer equation for polarized radiative transport in graded index media. J Quant Spectrosc Radiat Transf 113(3):239–250

Zhao JM, Tan JY, Liu LH (2013) A second order radiative transfer equation and its solution by meshless method with application to strongly inhomogeneous media. J Comput Phys 232(1):431–455

Zhou H-C, Cheng Q (2004) The DRESOR method for the solution of the radiative transfer equation in gray plane-parallel media. In: Mengüç MP, Selçuk N (eds) Proceedings of the fourth international symposium on radiative transfer, Istanbul, pp 181–190

Zhou H-C, Lou C, Cheng Q, Jiang Z, He J, Huang B, Pei Z, Lu C (2005) Experimental investigations on visualization of three-dimensional temperature distributions in a large-scale pulverized-coal-fired boiler furnace. Proc Combust Inst 30(1):1699–1706

Zhu K-Y, Huang Y, Wang J (2011) Curved ray tracing method for one-dimensional radiative transfer in the linear-anisotropic scattering medium with graded index. J Quant Spectrosc Radiat Transf 112(3):377–383